Unified theory of segregated-stack organic charge-transfer solids: Magnetic properties

S. Mazumdar
Center for Nonlinear Studies, Los Alamos National Laboratory, University of California, Los Alamos, New Mexico 87545 and GTE Laboratories Incorporated, 40 Sylvan Road, Waltham, Massachusetts 02254*

S. N. Dixit
Arthur Amos Noyes Laboratory of Chemical Physics, California Institute of Technology, Pasadena, California 91125
(Received 28 April 1986)

A theoretical description of the complete family of quasi-one-dimensional segregated-stack charge-transfer solids within a single model has remained elusive mostly because of the rich variety of behavior within the family. In particular, materials with both strongly enhanced as well as almost unenhanced static magnetic susceptibilities are known. Furthermore, a large number of different interpretations of the static magnetic susceptibility data have led to an intense controversy over the role of Coulomb correlations in these narrow-band systems. By comparing structurally similar materials with different magnetic behavior we show that (a) these differences do not originate in differences in molecular properties or crystal structures and (b) none of the simple electron-electron or electron-phonon coupled models can explain the observed differences in susceptibility behavior. Within a previously proposed extended Hubbard model we then show that the susceptibility is expected to vary strongly and systematically as a function of the degree of charge transfer. Detailed comparisons of both the magnitude of the high-temperature susceptibilities as well as the temperatures at which the susceptibilities peak for a large number of materials are made with theoretical predictions to prove the validity of our model. In addition we discuss how other properties of the complete family can be explained and predicted within the present model, and show that the parameters of the model can be obtained from charge-transfer absorption data. Several of the newly synthesized materials have been suggested to have weak electron correlations based on weakly enhanced susceptibilities and the absence of the $4k_F$ instability. We propose, however, that the above experimental features are consequences of the specific charge-transfer range within which these materials lie, and do not imply weak correlations.

I. INTRODUCTION

Quasi-one-dimensional organic charge-transfer (CT) solids have been of considerable recent interest[1–5] due to their potential technological use as organic electronic materials and their novel low-dimensional features. Despite the intense activity on these materials for more than a decade, the development of a unified theoretical description, which explains the behavior of the *complete* family of organic conductors, at least on a semiquantitative level, has been difficult. There are two principal reasons for this. First, the variety of electronic properties even among the segregated stack CT solids alone is remarkably rich. Structurally similar materials, with nearly identical molecular components and crystal structures, often exhibit very different behavior. Second, due to the extremely narrow bandwidths (0.5—1 eV) of these materials, direct Coulomb interactions between electrons,[6–9] intramolecular[10,11] and intermolecular[12–14] electron-phonon interactions, disorder[15–17] due to the random orientations of the dipole moments in asymmetric counterions or due to interrupted strands, can all influence electronic and magnetic behavior. Precisely because of the above, different theoretical models emphasizing different interactions have been common,[6–17] and any of these models explains at least certain features of a few materials, though often within a limited temperature range. This has led to a long-standing controversy over the role of Coulomb interactions in these narrow-band materials, as "experimental evidence" for both weak[18–23] and strong[7,12,24–28] Coulomb correlations has been found.

It is our opinion that the "true" theoretical model should be to explain the behavior of the *complete* family of segregated-stack CT solids. In particular, it should explain the *differences* in behavior that are often observed between structurally similar compounds. The particular properties of CT solids we are interested in are the static magnetic susceptibility, the various phase transitions that occur at low temperatures, and both low- and high-frequency optical properties. The magnetic susceptibilities of a very large number of materials are strongly enhanced over the theoretical Pauli values, and this has been cited as evidence for both strong Coulomb interaction between electrons[7] as well as of a strong band-narrowing effect (within a weak correlation model) due to electron-phonon interactions.[29] However, a smaller but significant number of materials exhibit unenhanced or weakly enhanced susceptibilities,[5,18,20–23,30–35] and the reason for this difference is not obvious from the above simple theoretical ideas of electron-electron or electron-phonon coupling. Indeed, the magnetic behavior of this latter class of materials has often been cited as evidence

for weak electronic correlation in *all* the CT solids.[36] Similar problems exist with the phase transitions in these solids. In usual quasi-one-dimensional systems, such phase transitions are due to formation of density waves with periodicity $2k_F$, where k_F is the Fermi wave vector within a one-electron picture. In the organic solids, however, several systems undergo phase transitions leading to density waves with periodicities $4k_F$, while others which undergo only the "normal" $2k_F$ Peierls transition are also known.[5,21,25,37,38] Furthermore, the temperatures at which these transitions occur can also be widely varying. Similarly, several anomalies in optical behavior also are known, and a consistent theory should be able to explain all of the above anomalies.

In this series of papers we develop such a unified description of these organic solids. Brief presentations of these ideas were made earlier.[39,40] The particular experimental quantity we will be interested in here is the magnetic susceptibility, which has been a source of intense controversy. A complete description of the phase transitions requires detailed studies of the several different broken symmetries that are possible in one dimension and that can often coexist.[8,40–42] The results of these investigations of broken symmetries will be published later.[43] Here we only mention that the conclusions of these investigations on one-dimensional broken symmetries are in complete agreement with the present study of magnetic behavior. Similarly, we avoid discussing the full range of optical behavior at the moment, but only point out here (see the Appendix) that consistent values of electron correlation parameters can be obtained from the optical studies of materials that absorb at *different* frequencies.[6(c)] Our principal purpose is to demonstrate that *explicit* inclusion of both intramolecular and intermolecular electron correlations can successfully explain the observed systematics in magnetic behavior,[39] and the detailed examination of the latter for the complete family of CT solids leads naturally to the present theoretical model. Aside from the susceptibility, phase transitions, and optical behavior, transport behavior is also of interest. However, existing experimental data[1–5] indicate that the actual temperature dependence of the dc conductivity is strongly dependent on crystal structures and counterions, so that a unified description of transport behavior is considerably more difficult. In addition, we show in the present paper that the proper theoretical model for these materials involves strong Coulomb interactions between electrons, and transport theory for such correlated systems, particularly in the presence of disorder and charge-density waves, is nonexistent at present, although it may be possible to explain the behavior of a few materials within a relatively narrow temperature range.

In Sec. II we briefly review the experimental situation for the magnetic susceptibility, emphasizing the differences in the susceptibility behavior between structurally similar materials. We point out that such differences cannot be explained on the basis of differences in crystal structures, molecular properties, or bandwidths. We critically examine the simple electron-electron or electron-phonon coupled models proposed for these systems, and point out that all of these predict a nearly uniform magnetic behavior (i.e., uniformly enhanced or unenhanced susceptibility) for CT solids, in contradiction to the experimental observation. The requirement that the correct theoretical model should explain the observed differences leads naturally to the extended Hubbard Hamiltonian proposed for these systems,[6(c),39,40,42] as is then shown within a physically intuitive picture that predicts a systematic dependence of magnetic behavior on band filling, or more precisely, the degree of charge transfer ρ from the cations to the anions.[39,40] In Sec. III we present the results of finite chain calculations of magnetic susceptibilities as well as several different ground-state correlation functions as a function of ρ that are related to the magnetic susceptibility within our proposed theoretical model. Detailed comparison of experimental susceptibilities, in particular, enhancement factors (relative to the theoretical Pauli susceptibilities) and the temperatures at which the susceptibility maxima are reached is made in Sec. IV, and it is shown that the complete family of segregated-stack CT solids obeys our theoretical prediction. Finally, in Sec. V, we summarize our conclusions and discuss the implications of present results for other properties of CT solids.

II. REVIEW OF EXPERIMENTAL MAGNETIC SUSCEPTIBILITIES AND THEORETICAL MODELS

In this section we briefly review the experimental data for a few materials that have been studied the most and discuss predictions of several theoretical models. We have, for the present, chosen materials that are structurally similar and hence indicate the systematic dependence on ρ most clearly, although we later show this to be true for the entire family.

Probably the most well-studied susceptibility $\chi(T)$ as a function of the temperature T is that of tetrathiafulvalene-tetracyanoquinodimethane (TTF-TCNQ).[7,19,31,44] While there is still some disagreement over the relative bandwidths of the TTF and TCNQ chains,[44] it is generally agreed that the high-temperature $\chi(T)$ for TTF-TCNQ is highly enhanced over the theoretical Pauli susceptibility χ_P, where χ_P for a single chain is given by

$$\chi_P = \frac{N_0 \mu_0^2}{\pi \mid t \mid \sin(\pi\rho/2)} , \tag{1}$$

where μ_0 is the Bohr magneton, N_0 the Avogadro number, ρ the average number of electrons or holes per molecular site, and $\mid t \mid$ the one-electron nearest-neighbor hopping integral. It is known that the bandwidth parameter $\mid t \mid$ varies by as much as a factor of 2 in CT solids, but for our purpose we have chosen a uniform bandwidth $4 \mid t \mid$ of 0.5 eV for both donor and acceptor stacks in single-chain as well as two-chain materials. This is because our primary interest is in pointing out the systematic ρ dependence in materials with nearly the same bandwidths, and its implications for theoretical modeling. None of the conclusions reached here change even if the bandwidths are taken to be twice as large, and we shall devote additional discussions to selenium-based donor chains with wider bands ($4 \mid t \mid \sim 1$ eV). Similarly, we do not make distinctions between one-chain and two-chain

materials, since the very small interchain hopping can influence the magnetic behavior only at low temperatures where three-dimensional couplings become important, and our interest in the present paper will be limited to the high-temperature susceptibility. The enhancement factor $\chi_{\text{expt}}/\chi_P$ for TTF-TCNQ at room temperature, or at 350 K where $\chi(T)$ exhibits a peak, is nearly 3. Taken in isolation, this fact can be explained both within the simple electron-electron or electron-phonon coupled models. Let us review here the options.

The model emphasizing the electron-electron interaction and that has been used most widely is the simple Hubbard Hamiltonian,

$$H_{\text{Hubbard}} = U \sum_i n_{i\uparrow} n_{i\downarrow} + t \sum_{i,\sigma} (c_{i\sigma}^{\dagger} c_{i+1,\sigma} + c_{i+1,\sigma}^{\dagger} c_{i\sigma}) , \quad (2)$$

where $c_{i\sigma}^{\dagger}$ and $c_{i\sigma}$ are electron creation and annihilation operators for site i and spin $\sigma(=\uparrow,\downarrow)$, $n_{i\sigma}$ are the corresponding number operators, and U the on-site repulsion between two electrons. The implicit parameter in Eq. (2) is ρ, with $\rho=1$ corresponding to a magnetic semiconductor and all $\rho<1$ materials being conductors[45] even at $U/t\to\infty$. Equation (2) predicts enhanced $\chi(T)$ for all ρ, provided that $U/4t$ is large. CT absorption at ~ 1.0 eV as well as an activation energy of semiconduction [$\sim\frac{1}{2}(U-4t)$ within Eq. (1)] of 0.2–0.3 eV in $\rho=1$ materials[46] indicates $U\sim 1.0$ eV in $\rho=1$ systems. The experimental $|t|$ of 0.1–0.2 eV then justifies [within Eq. (2)] using the $U/t\to\infty$ approximation for the magnetic behavior of CT solids with arbitrary ρ, which is that of a Heisenberg spin Hamiltonian H_{spin} within this limit[45]

$$H_{\text{spin}} = J \sum_i \mathbf{S}_i \cdot \mathbf{S}_{i+1} , \quad (3)$$

where

$$J = \frac{2t^2}{U} \rho \left[1 - \frac{\sin(2\pi\rho)}{2\pi\rho} \right] . \quad (4)$$

Inclusion of disorder in Eq. (2) leads to a random exchange spin Hamiltonian,[47] which has been used to explain $\chi(T)$ behavior of materials of the type Qn(TCNQ)_2,[47,48] Ad(TCNQ)_2,[47,48] $\text{(NMP)}_x\text{(Phen)}_{1-x}\text{(TCNQ)}$,[49] etc., with asymmetric cation molecules. Note that such random exchange Heisenberg Hamiltonians assume the "large-U" model.

A long-standing controversy has, however, persisted over the magnitude of U in Eq. (2). While it is generally agreed that U for $\rho=1$ is large, it has often been argued that metallic screening in the conductors should lower U considerably, and various "small-U" approaches are common. However, this claim has not been proved either theoretically or experimentally, and with regard to screening, we strongly believe in the opinion expressed by Hubbard,[9(c)] viz., screening effects "will emerge in the solution of the problem posed by the Hamiltonian we start with and are not to be taken into account separately in setting up this Hamiltonian." Unlike Hubbard, however, we do not attempt to derive the correlation parameters, but simply get them from experiments. As we shall see, the screening does indeed emerge in the solution of the problem, in the form of increased or reduced values of the correlation functions of the type $\langle n_{i\uparrow} n_{i\downarrow} \rangle$ or $\langle n_i n_j \rangle$, but *not* in reduced values of the parameters in the Hamiltonian.

A more serious problem with the model emphasizing strong electron correlation is the unenhanced or weakly enhanced $\chi(T)$ found in many systems, which would suggest a "small-U" picture within Eq. (2). For instance, in comparing the experimental $\chi(T)$ of TTF-TCNQ, TSF-TCNQ, and HMTTF-TCNQ, Tomkiewicz *et al.* concluded that "the donor stack susceptibility is enhanced only in TTF-TCNQ" and that $\chi_{\text{expt}}/\chi_P$ are widely different even for the TCNQ chains.[31(a)]

Since, in principle, such differences can result from both differences in molecular properties that reduce the on-site electron correlation as well as differences in bandwidths originating from differences in crystal structures, we compare here three different compounds to show that neither of the two above reasons can explain the seemingly anomalous behavior. The materials we choose are TTF-TCNQ, TMTTF-TCNQ, and HMTTF-TCNQ, with $\chi_{\text{expt}}/\chi_P$ at high temperatures being 2.8–3.0,[7] 2.3–2.4,[18] and 1.1–1.3,[31(a)] respectively. The donor molecules are nearly the same in all cases and hence the molecular U should be very close. Even if the argument is made that methylene groups in the HMTTF pull charges away from the center of the molecule (thus reducing U),[31(a)] similar arguments should be true for the TMTTF molecule too. Thus certainly any slight difference in molecular U cannot explain the difference in $\chi_{\text{expt}}/\chi_P$. In Table I we compare the relevant crystal structure parameters[50–52] for the three solids, and it is obvious from the nearest-neighbor distances and overlap patterns that both donor and acceptor stack bandwidths are nearly the same in these materials. Indeed, if the differences in $\chi(T)$ behavior were due to small differences in the bandwidth parameter in Eq. (2), one would have expected from Table I that TTF-TCNQ would have the largest bandwidth and hence the most weakly enhanced χ. Finally, all of the above materials are highly anisotropic,[18] and weak interchain transfers cannot explain the factors of 2–3 difference in $\chi_{\text{expt}}/\chi_P$.

As we shall show in Sec. IV, the same conclusions are reached by comparison of other materials with structural similarities. Here we only mention the case of the alloy series $\text{(NMP)}_x\text{(Phen)}_{1-x}\text{(TCNQ)}$, $0.5\le x\le 1$, in which neutral phenazine (Phen) molecules are substituted for the donor NMP molecules,[49] such that ρ in the TCNQ chain varies from 0.5 to 0.67 [CT from NMP to TCNQ becomes progressively more incomplete as x increases from 0.5 (Ref. 49)]. While there are some questions regarding material purity[53] as well as the nature of defects[40] around $x\to 0.5$ ($\rho\to 0.5$), χ_{expt} at 300 K decreases rapidly with x except for a small region around $x=0.5$. Again, this is in contradiction to the predictions of Eq. (2), within which only a weak ρ dependence is expected. In fact, NMP-TCNQ is a two-chain conductor with a total susceptibility at 300 K *lower* than the single-chain conductor $\text{(NMP)}_{0.5}\text{(Phen)}_{0.5}\text{(TCNQ)}$.

An alternate theoretical model that has also been used to explain enhanced $\chi(T)$ claims that U is small

TABLE I. Relevant crystal structure parameters that determine the one-electron bandwidth parameters for three representative CT solids. The angle between the normal to the molecular plane and the stack axis determines the overlap pattern between molecular orbitals on nearest neighbors. The abbreviations in the compound column are as follows: TCNQ, tetracyanoquinodimethane; TTF, tetrathiafulvalene. The prefixes TM and HM stand for tetramethyl and hexamethylene, respectively.

Compound	D-D distance (in Å) along stack axis	A-A distance (in Å) along stack axis	Angle between normal to the molecular plane and stack axis, donor chain[a]	Angle between normal to the molecular plane and stack axis, acceptor chain[a]
TTF-TCNQ	3.47	3.17	24.5°	34°
TMTTF-TCNQ	3.53	3.27	23.2°	32.2°
HMTTF-TCNQ	3.57	3.25	23.8°	34.2°

[a]The dihedral angles between donor and acceptor molecules in TTF and TMTTF-TCNQ (58.5° and 55.4°) are much larger than the dihedral angle in HMTTF-TCNQ (10.4°); while this affects the relative magnitudes of interchain overlaps, the intrachain bandwidth is a function of only the distances and angles presented here.

(screened), and the dominant interaction of the band electrons is with the phonons in the system.[29] Since linear electron-phonon coupling would always lead to a bound polaron, the quadratic electron-phonon coupling is emphasized within the model Hamiltonian,

$$H_{e\text{-ph}} = t\sum_i (c_i^\dagger c_{i+1} + \text{H.c.}) + \hbar\omega \sum_i (a_i^\dagger a_i + \tfrac{1}{2}) + \sum_{i,j} g^{(2)}(i+j) c_i^\dagger c_i (a_j^\dagger + a_j)^2 , \quad (5)$$

where c_i and a_i correspond to electron and phonon operators (note that spin is irrelevant here), ω the phonon frequency, and $g^{(2)}$ the quadratic electron-phonon coupling constant. Within Eq. (5), the enhancement of χ is due to the standard band-narrowing effect due to strong electron-phonon coupling, an effect that would be observed even if a strong linear electron-phonon coupling is used instead of the quadratic coupling. The quadratic electron-phonon-coupling model, in principle, also explains the $4k_F$ instability[54] as well as the approximately T^2 dependence of dc conductivity[29] in materials of TTF-TCNQ type, and these aspects will be discussed in a later publication. Once again, the weakness of Eq. (5) *and* other similar electron-phonon-coupled models is the same as for the simple Hubbard Hamiltonian in Eq. (2), viz., they predict a nearly universal behavior (enhanced χ) for all CT solids, unless very different electron-phonon couplings are used for different compounds. We have already seen that the crystal structures of TTF-TCNQ, TMTTF-TCNQ, and HMTTF-TCNQ indicate nearly identical donor and acceptor chain bandwidths, and there is no reason to assume that the electron-phonon couplings (linear or quadratic, intramolecular, or intermolecular) are very different. For the same reason other related electron-phonon-coupled models[36] for the enhanced χ can be discounted, although as we discuss later, the actual temperature dependences of χ may very well be related to the various distortions that arise from electron-phonon interactions.

Finally, a third model that has been used often is the Wigner crystal model of Kondo and Yamaji[9(b)] and Hubbard,[9(c)] who pointed out the very important role of *intersite* Coulomb interactions in these systems (see also Refs. 6 and 7 for discussions of intersite interactions). According to these authors, CT solids are described by the Hamiltonian,

$$H_{\text{Wigner}} = H_{\text{Hubbard}} + \sum_{i,j} V_j n_i n_{i+j} , \quad (6)$$

where H_{Hubbard} is the Hamiltonian in Eq. (2), n_i is the total number of electrons in site i, and V_j are the repulsions between electrons j sites apart. According to Hubbard's estimates $U = 2.9$ eV, $V_1 = 0.9$ eV, and even V_4 is comparable to or larger than t. Ground-state solutions to Eq. (6) were obtained[9(c)] for the limit $U = \infty$ and $t = 0$, which was considered to be a valid limit for such a large value of U and relatively small t, and where the model becomes equivalent to an Ising model with long-range interactions in the presence of a magnetic field.[55] Without going into further details, it suffices to say that the $U = \infty$ limit precludes all double occupancies and therefore again predicts universally enhanced χ (actually Curie susceptibility), in contradiction to experiments. Furthermore, the magnitudes of U, V_j, etc. estimated by Hubbard are larger than all other estimates by factors of 2 to 3, and also, such long-range interactions will obliterate the difference between various ρ even at finite U.

We have, in the above, discussed only those theoretical models that have been suggested as unified theoretical descriptions. Aside from the above, several more specific modified band-theoretical models thought to be applicable to particular systems (usually TTF-TCNQ) have also been suggested in the past.[56] We do not discuss these any further, since experimentally, the origin of at least the enhanced χ in various materials is the same, as has been discussed by numerous authors.[6,7,36]

In order to develop the "true" theoretical model for CT solids, we need to first understand why χ is enhanced at all by electron correlation. All the Hamiltonians discussed above conserve the total spin. Consider now two spin subspaces S and S', where $S < S'$. The maximum possible number of doubly occupied sites in subspace S is larger than the maximum number in S'. The number of

configurations is therefore larger in the subspace S, and relatively greater configuration interaction ensures that the energies of eigenstates within subspace S are much lower than those in subspace S' at small U. The extent of the above configuration interaction within any spin subspace depends only on the matrix elements of the Coulomb interaction part of the Hamiltonian for various configurations. Consider, for simplicity, two configurations *in real space* that are related by a single electron transfer and that differ by a double occupancy. Denoting by $H_{1,1}$ and $H_{2,2}$ the matrix elements of the Coulomb interaction part of the Hamiltonian for the two configurations, it is obvious that the configuration interaction increases as the difference $|H_{2,2}-H_{1,1}|$ decreases. Within the simple Hubbard Hamiltonian, $|H_{2,2}-H_{1,1}|=U$, and therefore as U is raised there is smaller configuration interaction, affecting the energy states of the lower spin subspaces more than those of the higher spin subspaces. The energy states within subspace S are raised more than those within subspace S' and χ becomes enhanced. The enhancement factor $\chi_{\text{expt}}/\chi_P$ therefore depends only on quantities like $|H_{2,2}-H_{1,1}|$, i.e., the net barrier to double occupancy. The latter, in its turn, not only determines thermodynamic quantities like $\chi(T)$, but also ground-state correlation functions like $\langle n_{i\uparrow}n_{i\downarrow}\rangle$ and $\langle S_i^z S_{i+j}^z\rangle$, where S_i^z is the zth component of the spin on site i. If we therefore believe that the parameter U/t is nearly equal in all materials (at least in those which are chemically and structurally equal), the simple Hubbard Hamiltonian cannot explain variable $\chi_{\text{expt}}/\chi_P$, for *any* value of U, *with or without electron-phonon interactions.*

To explain variable enhancements, we therefore need a variable U_{eff}, where U_{eff} is an *effective barrier to double occupancy.* This quantity can vary strongly as a function of ρ (Ref. 39) within the extended Hubbard Hamiltonian,

$$H_{\text{EH}}=H_{\text{Hubbard}}+V_1\sum_i n_i n_{i+1}\ , \tag{7}$$

where we have retained only the nearest-neighbor Coulomb repulsion V_1 in Eq. (6) and will retain a *finite* U. As we discuss in the Appendix, more distant interactions along the chain are negligible in real materials, although a weak second-neighbor interaction $V_2\sim t$ is possible. The ρ dependence of U_{eff} will be true for *any finite* U/V_1, but for the specific case of CT solids we believe $U\sim 1.2$—1.4 eV, $V_1\sim 0.3$—0.5 eV (see Appendix).

As suggested by Hubbard,[9(c)] we examine first the $t=0$ solutions to Eq. (7) for an intuitive understanding of the behavior of $U_{\text{eff}}(\rho)$. For all $\rho\leq 1$, the ground-state configuration in this limit consists of only singly occupied and empty sites, i.e., double occupancies are forbidden. Furthermore, each configuration is an eigenfunction of the Hamiltonian in this limit. The barrier to double occupancy is simply the energy difference between the ground-state configuration and a proper final configuration that has one double occupancy and is reached by a single nearest-neighbor hop. If several such configurations with different energies can be reached by nearest-neighbor electron transfers, the overall barrier to double occupancy is a weighted sum of all the energy differences, where the relative weight of each term is proportional to the probability of reaching the appropriate configuration. In Fig. 1, we present relevant ground-state configurations and configurations reached by single hops for $\rho=1$, $1-1/N$, 0.75, and 0.5. For $\rho=1$, the ground state at $t=0$ consists of all sites singly occupied, and any nearest-neighbor hop leads to a configuration at energy $U-V_1$, as shown in Fig. 1(a). $U_{\text{eff}}(\rho=1)$ is therefore $U-V_1$ in this limit. If we now remove an electron from any site i, the two particular electron transfers from sites $i\pm 2$ to sites $i\pm 1$, cost an energy only $U-2V_1$. The overall barrier to double occupancy is a function of both the probability of the low-energy transfer and its actual magnitude, and U_{eff} in this case is infinitesimally smaller than $U-V_1$. As more and more electrons are removed from the system, the relative weight of the low-energy transfers increases continuously, until it reaches a maximum at $\rho=0.75$, where half the transfers leading to double occupancies cost $U-2V_1$, as seen in Fig. 1(c). The ground-state configuration in Fig. 1(c) is degenerate with the configuration $\cdots 01101111\cdots$, where the numbers signify site occupancies, but even with this initial configuration one-third of all transfers leading to double occupancies are of the low-energy type. Further reduction in electron concentration removes the electrons which are at the centers of sequences of three occupied sites in Fig. 1(c), until at $\rho=0.5$ the ground state consists of alternately occupied sites. As seen in Fig. 1(d), the energy difference between the ground state and the final configuration with one doubly occupied site is now U itself. Furthermore, the final configuration here is reached by two hops instead of one, so that we expect $U_{\text{eff}}(0.5)$ to be actually *larger* than U.

The variation in $U_{\text{eff}}(\rho)$ is expected to persist at $t\neq 0$ for U, $V_1>t$, and finite U/V_1. Based on the above discussion for the $t=0$ limit, we can therefore construct the schematic plot of $U_{\text{eff}}(\rho)$ versus ρ,[39] shown in Fig. 2. The relative magnitude of U_{eff} and the bandwidth $4t$ is of course dependent on the actual values of U/t and V_1/t, and our conclusion that $U_{\text{eff}}\lesssim 4t$ for $0.6\lesssim\rho\lesssim 0.8$ is based on comparison with experimental magnetic susceptibilities and numerical calculations with U/t and V_1/t close to

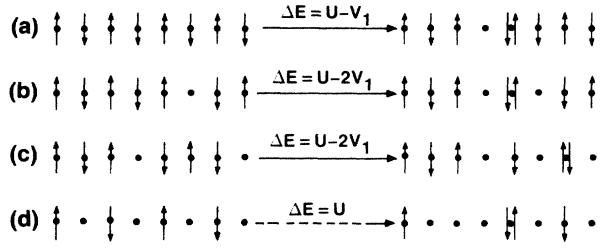

FIG. 1. Relevant many-electron configurations that determine $U_{\text{eff}}(\rho)$ within the extended Hubbard model, near $t\to 0$ limit, for several different ρ. In each case, the initial configuration is the ground-state configuration, while the final configuration contains one doubly occupied site and is reached from the former by a single nearest-neighbor electron transfer (except $\rho=0.5$, where the final configuration requires *two* nearest-neighbor transfers; the dashed arrow in the figure denotes such a concerted two-step process).

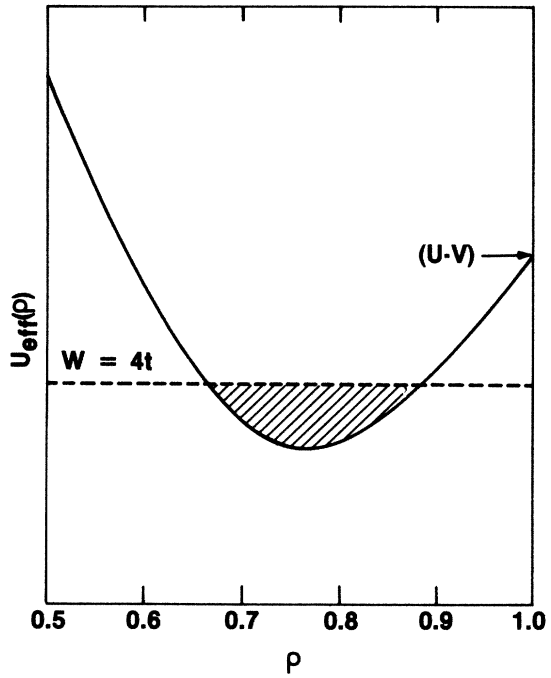

FIG. 2. Schematic behavior of $U_{\rm eff}(\rho)$ vs ρ for a single chain. Interchain interactions are now expected to alter the behavior qualitatively (see text).

values suggested by optical-absorption measurements in TTF- and TCNQ-based solids.

In the next section we present results of our numerical calculations. A few additional points are made here, however. Firstly, $U_{\rm eff}$ is a measure of the overall barrier to double occupancy, and therefore of only the on-site correlation $\langle n_{i\uparrow}n_{i\downarrow}\rangle$. It is expected to reproduce quantities like $\chi(T)$ *but not* other observables that depend on long-range correlations (e.g., the structure factor); however, it can still *indirectly* determine the nature of the long-range correlations and whether $2k_F$ or $4k_F$ charge-density waves are favored in a given case (see Sec. V and Ref. 40). This is because within a linear electron-phonon-coupled model the $4k_F$ charge-density wave always requires a small $\langle n_{i\uparrow}n_{i\downarrow}\rangle$. Secondly, even if $U_{\rm eff}\lesssim 4t$ for $0.6\lesssim\rho\lesssim 0.8$, we do not imply that these systems are uncorrelated, but rather that the *nature* of the correlations are different. Both these points are further discussed in Secs. III and IV.

III. NUMERICAL RESULTS FOR $\chi(T)$ AND GROUND-STATE CORRELATION FUNCTIONS

The ρ dependence we conjecture from intuitive reasoning is expected to become weaker for finite bandwidth. In order to demonstrate the considerable strength of this dependence for realistic values of correlation parameters we have performed exact numerical calculations, in the absence of analytical results for the many-body Hamiltonians discussed in Sec. II. Our estimates of the correlation parameters are $U\sim 1.2$–1.4 eV, $V_1\sim 0.3$–0.5 eV. These values are obtained from fits to the experimental charge-transfer absorption spectra, as discussed in the Appendix, where we compare the spectra of materials at the two extreme densities, $\rho=0.5$ and 1. Even though the two classes of materials absorb at very different frequencies, they yield the same values for U and V_1, thus giving us confidence in these estimates. We have assumed a bandwidth $4t\sim 0.5$ eV, and present numerical results for $U=7\sqrt{2}t$ and $8\sqrt{2}t$, $V_1=2\sqrt{2}t$ and $3\sqrt{2}t$. In addition, we have performed our calculations also with a weak but nonzero V_2. For selenium-based donor chains a bandwidth of ~ 1.0 eV has been suggested, and this would require smaller U/t and V_1/t (but nearly the same U/V_1, leading, again, to a strong ρ dependence within this family). None of the results obtained here are qualitatively affected, except that larger bandwidths simply imply slightly larger $\langle n_{i\uparrow}n_{i\downarrow}\rangle$. However, these larger on-site correlation functions still do not justify using band-theoretical models.

The most direct way to verify the intuitive arguments of Sec. II is to calculate magnetic susceptibilities $\chi(T)$. This was done numerically for systems of $N_e=4$ electrons distributed over $N=4$, 5, 6, 7, and 8 lattice sites, corresponding to $\rho=1$, 0.8, $\frac{2}{3}$, 0.57, and 0.5. Due to the finite energy gaps in such finite systems we do not expect convergence in $\chi(T)$ at low T, but our interest is only in the high-temperature part of the susceptibility. There are by now numerous demonstrations of the convergence of thermodynamic properties at high T of one-dimensional systems with short-range interactions.[57] The numerical calculations of $\chi(T)$ were done for open chains only, since finite undistorted $4n$-electron periodic rings have a ground-state total spin $S=1$ instead of $S=0$ for $N_e\neq N$. For better comparison with the infinite system we have therefore assumed an interaction V_1 between sites 1 and N. We have verified that the behavior of $U_{\rm eff}(\rho)$ remains unaltered even if $V_{1,N}=0$.

For comparison of various ρ we first calculate $\chi(T)$ from Eq. (7) with fixed U and V_1, and then compare it with $\chi(T)$ obtained from the simple Hubbard Hamiltonian [Eq. (2)] with an on-site repulsion $U_{\rm eff}=U-V_1$. Finally, by trial and error, we find the effective repulsion $U_{\rm eff}$ that best reproduces the $\chi(T)$ obtained from Eq. (7). Our results for $\rho=1$, 0.8, and 0.57 are shown in Fig. 3 for one set of U and V_1. The results for all other U and V_1 are similar. For $\rho=1.0$, $U_{\rm eff}\sim U-V_1$, as can be guessed from perturbative results near $t\rightarrow 0$. For $\rho=0.8$, $U_{\rm eff}$ is found to be much *smaller* than $U-V_1$ while for $\rho=0.57$ $U_{\rm eff}>U-V_1$ and is comparable to U itself. For $\rho=0.5$ (not shown here), $U_{\rm eff}$ is even larger and is greater than U, as might be expected from the arguments given in Sec. II. Besides the magnitudes of the susceptibility the temperatures $T_{\rm max}$ at which the maxima of $\chi(T)$ in Fig. 3 occur are also of interest. Within the simple Hubbard Hamiltonian with a fixed on-site repulsion, the maxima occur at comparable temperatures for all ρ [the slight differences in $T_{\rm max}$ are due to the weak ρ dependence of the exchange integral in Eq. (4)], while within the extended Hubbard Hamiltonian we find that $T_{\rm max}$ is much smaller for $\rho=0.57$ than it is for $\rho=0.8$. This is to be expected within perturbation theory, the Heisenberg exchange integral $J_{\rm eff}(\rho)$ being proportional to $2t^2/U_{\rm eff}(\rho)$, and

$kT_{\max} \cong 1.282 J_{\text{eff}}(\rho)$.[57] As we point out in the next section, not only $\chi_{\text{expt}}/\chi_P$ but also the experimental $T_{\max}$ obey this predicted trend.

Even the above limited set of results clearly points toward a systematic trend.[39] In order to probe this behavior further [in particular, to demonstrate the smooth behavior of $U_{\text{eff}}(\rho)$] it is necessary to extend the calculations to larger systems and a larger number of densities. In practice, however, the Hamiltonian matrices become too large for $N_e > 4$ and all but the smallest N (especially for $0 < S < N_e/2$), so that it is extremely difficult to obtain the complete energy spectrum and the thermodynamic behavior. We point out, however, that this is not necessary as several ground-state correlation functions are directly related to the thermodynamics. As discussed in the preceding section, enhancement of χ is dependent on the overall energy barrier to double occupancy, which in turn determines the normalized *ground-state* probability of double occupancy or the pair correlation function $g(\rho)$ on the same site, defined as,

$$g(\rho) = \frac{\langle n_{i\uparrow} n_{i\downarrow} \rangle}{\langle n_{i\uparrow} \rangle \langle n_{i\downarrow} \rangle} \tag{8a}$$

$$= \frac{4\langle n_{i\uparrow} n_{i\downarrow} \rangle}{\rho^2} . \tag{8b}$$

The smaller the $g(\rho)$, the more enhanced is $\chi(T)$ and the smaller the $T_{\max}$. An additional quantity that is related to $\chi(T)$ behavior is the "spin structure factor" $S_\sigma(q)$, defined as

$$S_\sigma(q) = N^{-1} \sum_{l,j} \langle S_l^z S_{l+j}^z \rangle e^{iqja} , \tag{9}$$

where S_l^z is the z component of the spin on site l, q is a wave vector, and the expectation value is for the ground state only. The tendency towards antiferromagnetism is seen from a peak in $S_\sigma(q)$ at $q = 2k_F = \rho\pi/a$, where a is the lattice constant; the more intense the peak, the more enhanced χ is.

The fact that the simple Hubbard Hamiltonian will yield a nearly uniform $g(\rho)$ is seen most easily in the two limits of $U = 0$ [$g(\rho) = 1$ for all ρ] and $U = \infty$ [$g(\rho) = 0$ for all ρ]. This conclusion remains unchanged even when electron-phonon couplings are included. We have numerically evaluated $g(\rho)$ for $N_e = 6$ and $N = 6,7,8,9,10,11,12$; $N_e = 8$, $N = 8,10,11,12$; and $N_e = 10$, $N = 10$; thus covering $\rho = 1$, 0.857, 0.80, 0.75, 0.727, 0.67, 0.6, 0.545, and 0.5. All of the above calculations were done for closed periodic rings for which convergence is faster than for open chains. Also, we compare here only ground-state properties, which are expected to converge for the tight-binding case for the above ring sizes. Rather good estimates of finite-size effects can be obtained from the data which include two different ρ for which the calculations were performed with multiple ring sizes ($N = 6,8,10$ for $\rho = 1.0$ and $N = 9,12$ for $\rho = 0.67$). Similar estimates are also obtained from comparisons of $\rho = 0.727$ ($N = 11$), $\rho = 0.75$ ($N = 8$), and $\rho = 0.8$ ($N = 10$). In all cases finite-size effects are found to be small. Finally, the above calculations of $g(\rho)$ were also done for much larger systems ($N \sim 32$) using an extended projector quantum Monte Carlo method.[58] From the above calculations we verified that (i) smooth and continuous $g(\rho)$ behavior is obtained for each N_e by varying N; (ii) the absolute magnitudes of $g(\rho)$ depend weakly on N_e, and have converged to a few percent of the limiting values at $N \sim 10$; and (iii) most importantly, while the $g(\rho)$ plots are slightly different for each N_e, the overall qualitative behavior of $g(\rho)$ as a function of ρ is independent of N_e. Due to the nearly identical values of $g(\rho)$ obtained from the exact and

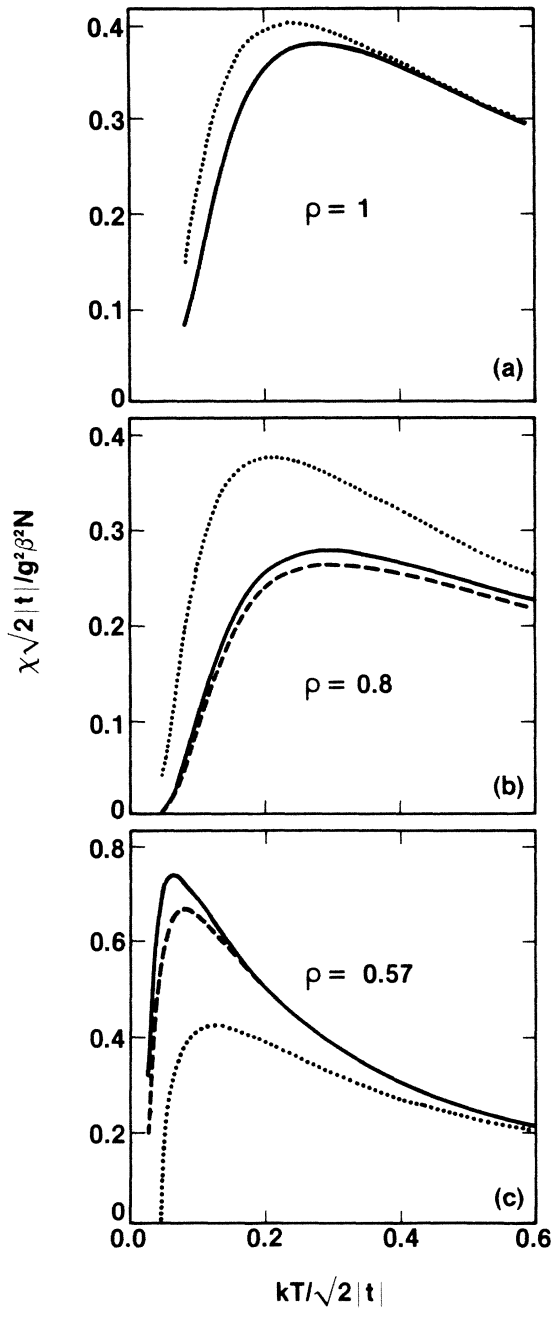

FIG. 3. Reduced magnetic susceptibilities versus reduced temperature for single chains of N molecules with $U = 7\sqrt{2}t$, $V_1 = 3\sqrt{2}t$, and $\rho = 4/N$. Solid line, Eq. 97). Dotted line, Eq. (2) with $U_{\text{eff}} = U - V_1$. Dashed line, Eq. (2) with (b) $U_{\text{eff}} = U - 1.6V_1$ and (c) $U_{\text{eff}} = U$.

Monte Carlo calculations, we present only the data obtained from the former.

Our results for the two values of U/t and V_1/t chosen here are shown in Figs. 4(a)–4(d). In Figs. 4(a) and 4(b) we plot $g(\rho)$ versus ρ for (i) the extended Hubbard model, (ii) the simple Hubbard model with effective on-site repulsion $U-V_1$, and (iii) the simple Hubbard model with on-site repulsion U. The simple Hubbard model yields a nearly ρ-independent $g(\rho)$ in all cases. For the extended Hubbard model, $g(1)$ in all cases is reproduced by $U_{\text{eff}}=U-V_1$, as expected, while for $\rho\rightarrow 0.5$ it is seen that $g(\rho, V_1\neq 0)<g(\rho, V_1=0)$, thus indicating again that $U_{\text{eff}}>U$ in this region. For intermediate ρ, in particular for $\frac{2}{3}<\rho<0.8$, $g(\rho)$ is considerably larger for $V_1>0$ and can be reproduced within an effective Hubbard model with $U_{\text{eff}}\lesssim 4t$ (but much larger than zero). A nonzero V_1 can therefore both decrease and increase $g(\rho)$, and the actual behavior depends very strongly on ρ itself. The effect of nonzero V_2 on $g(\rho)$ is shown in Figs. 4(c) and 4(d). In general, V_2 makes the ρ dependence weaker, but as seen in the figures, $g(\rho)$ can still be strongly varying. Furthermore, there is an upper limit on any realistic estimate of V_2, since within our model the nearest-neighbor repulsion is the driving force behind the $4k_F$ charge-density wave (CDW).[40,42]

As mentioned above, the behavior of the spin structure

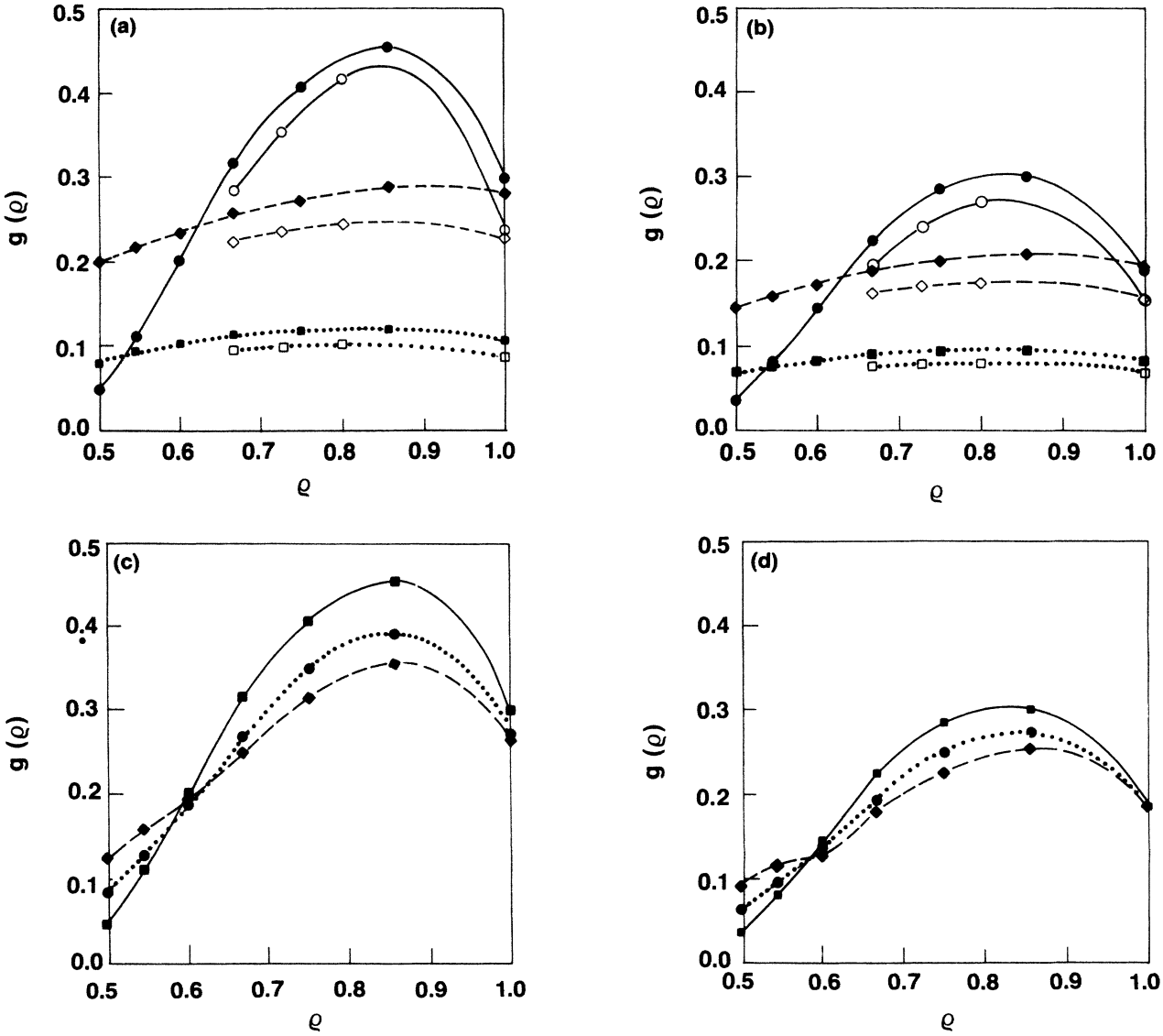

FIG. 4. The normalized probability of double occupancy $g(\rho)$ vs ρ for several cases. In each case the solid circles, solid diamonds and solid squares correspond to $N_e=4n+2=6$, while the open circles, open diamonds, and open squares correspond to $N_e=4n=8$. Calculations with larger N_e indicate that the $N_e\rightarrow\infty$ curve is bounded by the $N_e=4n$ and $N_e=4n+2$ curves in each case. (a) Solid line: $U=7\sqrt{2}t$, $V_1=3\sqrt{2}t$; dashed line: $U=4\sqrt{2}t$, $V_1=0$; dotted line: $U=7\sqrt{2}t$, $V_1=0$. (b) Solid line: $U=8\sqrt{2}t$, $V_1=3\sqrt{2}t$; dashed line: $U=5\sqrt{2}t$, $V_1=0$; dotted line: $U=8\sqrt{2}t$, $V_1=0$. (c) and (d) show the effect of nonzero V_2 on $g(\rho)$ for $V_1=3\sqrt{2}t$ and (c) $U=7\sqrt{2}t$, (d) $U=8\sqrt{2}t$. In both cases, the solid, dotted, and dashed lines correspond to $V_2/\sqrt{2}t=0$, 0.5, and 1, respectively. Note that the tendency of $g(\rho)$ to be flat for large V_2 is largest near $\rho\rightarrow 0.5$.

factor $S_\sigma(q)$ is a direct measure of the tendency towards antiferromagnetism and hence of enhanced χ, since there is no magnetic gap in one dimension. For the noninteracting band ($U=V_1=0$), $S_\sigma(q)$ increases linearly with q up to $q=2k_F$, while between $q=2k_F$ and $q=\pi/a$, $S_\sigma(q)$ is q independent. In Fig. 5 we show numerical results for $S_\sigma(q)$ for a large number of ρ. In order that the enhancements or suppressions of $S_\sigma(q)$ by V_1 are more visible, we have actually plotted the enhancement $\Delta S_\sigma(q)$ due to electron correlation, defined by

$$\Delta S_\sigma(U,V_1,q)=S_\sigma(U,V_1,q)-S_\sigma(0,0,q)\ . \tag{10}$$

For the noninteracting limit $\Delta S_\sigma(q)$ versus q is the x axis itself. For each ρ we show our results for (i) $U=7\sqrt{2}t$, $V_1=0$, (ii) $U=7\sqrt{2}$, $V_1=3\sqrt{2}t$, (iii) $U=4\sqrt{2}t$, $V_1=0$. It is seen that U alone enhances the $2k_F$ spin-density wave (SDW) in all cases, but the effect of nonzero V_1 is very strongly ρ dependent. Once again for $\rho=1$ the extended Hubbard model can be replaced with a simple Hubbard Hamiltonian with $U_{\text{eff}}=U-V_1$. For $\rho=0.75$ we find that the $2k_F$ SDW is suppressed much more strongly by V_1, while for $\rho=0.5$ and 0.6 the effect of V_1 is opposite and the SDW is *enhanced* by nonzero V_1, the enhancement for $\rho=0.5$ being very strong. While we show

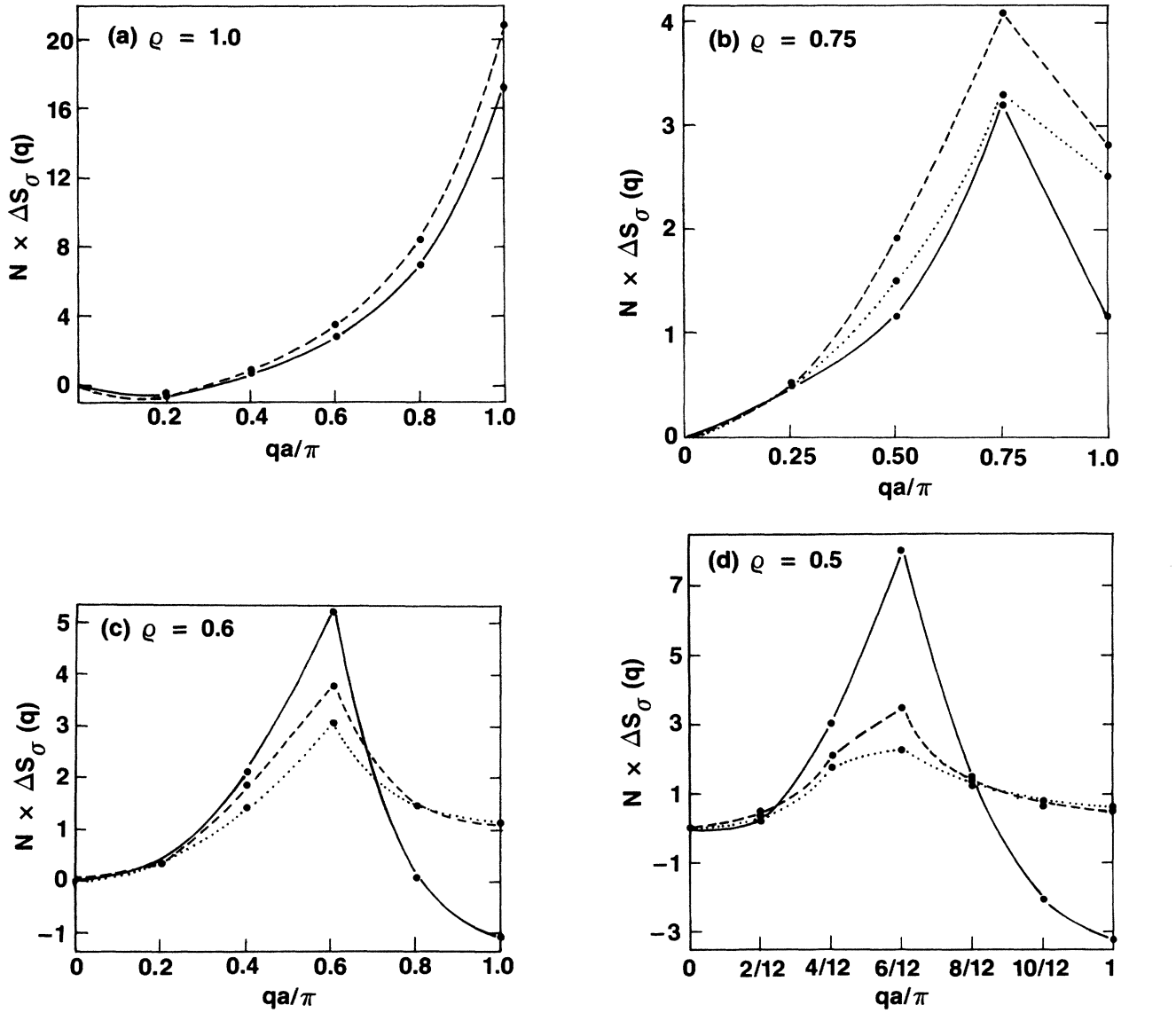

FIG. 5. Enhancement $\Delta S_\sigma(q)$ of the "spin structure factor" versus the wave vector q for several different ρ. In each case the enhancement is being measured with respect to the uncorrelated limit (see text). Solid line: Eq. (7) with $U=7\sqrt{2}t$, $V_1=3\sqrt{2}t$. Dotted line: Eq. (2) with $U=4\sqrt{2}t$, $V_1=0$. Dashed line: Eq. (2) with $U=7\sqrt{2}t$, $V_1=0$. The dotted line and the solid line are indistinguishable on the scale shown here for $\rho=1.0$, as is expected. $\Delta S_\sigma(q)$ peaks at $2k_F$ in all cases, but the effect of V_1 is seen to be strongly dependent on ρ (see text). The small negative value of $\Delta S_\sigma(q)$ near $q\to 0$ in (a) is a characteristic of all large N_e systems [$N_e=10$ in (a) but $N_e=6$ in (b), (c), and (d)], while the large negative values of $\Delta S_\sigma(q)$ for $q>2k_F$ in (c) and (d) are due to the very strong SDW amplitudes due to nonzero V_1 in this region of ρ.

representative results for only one combination of U and V_1, it should be obvious that similar effects would be seen for all realistic U and V_1. For unrealistically large V_1 the ρ dependence is even qualitatively different: the $2k_F$ SDW for a fixed U disappears now at a critical nearest-neighbor interaction $V_1^c > \frac{1}{2}U$ for $\rho=1$, while the SDW is enhanced at $\rho=0.5$ for all $V_1 < U$. For intermediate ρ ($\frac{2}{3} < \rho < \frac{3}{4}$), the disappearance of the $2k_F$ SDW occurs at $V_1^c(\rho) > \frac{1}{2}U$ [$V_1^c(\frac{3}{4}) = \frac{3}{4}U$, $V_1^c(\frac{2}{3}) = U$].

Our predictions for magnetic susceptibility of CT solids are then as follows. We expect a very strongly enhanced $\chi(T)$ for $\rho \to 0.5$, followed by a smooth reduction in the enhancement factor $\chi_{\text{expt}}/\chi_P$ until for $\frac{2}{3} < \rho < 0.8$ only small enhancement factors are observed. The region $0.6 < \rho < \frac{2}{3}$ is a transition region where both large and small enhancement factors may be observed, depending on the actual bandwidths, crystal structures, and molecular properties. Materials with $0.85 < \rho < 1$ are unknown, but here we expect $\chi_{\text{expt}}/\chi_P$ to increase again, until finally at $\rho=1$ we have a Mott-Hubbard semiconductor with strongly enhanced χ (the enhancement factor here, however, is expected to be smaller than it is for $\rho \to 0.5$). For $\rho > 1$, the behavior can be understood from electron-hole symmetry (see Sec. IV for a discussion of a real material in this range).

IV. COMPARISON WITH EXPERIMENTS

In the present section we compare our theoretical predictions to the experimentally observed magnetic susceptibilities of CT solids. The particular quantities we are interested in are $\chi_{\text{expt}}/\chi_P$ and $T_{\max}$.

For χ_{expt} we have taken the highest experimentally observed spin susceptibilities. For most materials the maximum experimental temperature is 300 K, and if the susceptibility is still rising at 300 K we have taken $\chi(300)$ as χ_{expt}. If, however, $\chi(T)$ exhibits a peak at some T, we consider the maximum susceptibility $\chi_{\max}$ as χ_{expt}, as indeed we should. Thus for cases where $T_{\max} > 300$ K, our values of enhancement factors are lower limits for the true enhancement factors. However, as we have pointed out in Sec. III, $T_{\max}$ itself is a criterion of weak or strong U_{eff}, and we predict the smallest $T_{\max}$ near $\rho=0.5$. We calculate the theoretical χ_P from Eq. (1) by assuming a uniform bandwidth of 0.5 eV and a free-electron g value. Since g-value decompositions of χ have not been done for most of the materials we list below, we do not attempt to determine individual donor and acceptor chain contributions χ_D and χ_A to the total spin susceptibility, but simply assume $\chi = \chi_D + \chi_A$, $\chi_D = \chi_A$. Neither this assumption nor the assumption of a uniform bandwidth is valid for all the materials, but here our basic motivation is to prove the validity of the extended Hubbard Hamiltonian as a universal theoretical model for CT solids by pointing out the systematic trend in χ that cannot be explained within any of the other existing models.

For the same reason as above, we do not attempt to fit the temperature dependence of $\chi(T)$. This is considerably more difficult. Firstly, $\chi(T)$ behavior at low temperature is strongly dependent on thermal contractions as well as the temperatures at which phase transitions occur. At temperatures below a phase transition which generates a magnetic gap, $\chi(T)$ is expected to go to zero. At slightly higher temperatures one is usually still in the one-dimensional fluctuation regime, and $\chi(T)$ is expected to increase rapidly, as indeed is found in nearly all cases. Secondly, and sometimes more importantly, it has been found that the degree of charge transfer in the same material can vary with temperature. For example, in TTF-TCNQ ρ decreases from 0.59 to 0.55 between low temperatures and room temperature;[59] similarly, for DBTTF-$TCNQCl_2$ ρ decreases from 0.55 to 0.52.[60] Since theoretically we predict larger χ for smaller ρ, such variations in ρ add to the steep behavior of $\chi(T)$. This particular factor has not been considered before but we consider this to be at least as important as the other factors that lead to a steep $\chi(T)$ variance with T. Finally, the zero-temperature susceptibility $\chi(0)$ is not known for the extended Hubbard model, and therefore extrapolations of numerical finite chain data, even if they were available for the complete CT range, are not possible. On general theoretical grounds, we expect, however, the T dependence to be approximately that of a Heisenberg chain for $\rho \to 0.5$, where we have seen that the nearest-neighbor interaction V_1 further enhances the decoupling between orbital and spin degrees of freedom for a strong U. Indeed, $\chi(T)$ behavior for several materials with CT near this region have been fitted to the Heisenberg model with phenomenological exchange integrals (and disorder parameters, when appropriate). For ρ appreciably larger than 0.5, but less than 1, however, we have seen that such decoupling does not occur and T dependence is more complicated. It may be possible that $\chi(0)$ here is close to that obtained from a simple Hubbard model with the appropriate $U_{\text{eff}}(\rho)$, but this requires further investigation. Due to the strong coupling between orbital and spin degrees of freedom in $\rho > \frac{2}{3}$, $T_{\max}$ here is much larger than $T_{\max}(0.5)$ in general, and therefore we compare also the experimental $T_{\max}$ as a function of ρ.

We have surveyed the experimental literature for $\chi(T)$ data, and in Table II we list our findings in order of increasing ρ, with the exception of NMP-TCNQ and TMTSF-DMTCNQ, which occur immediately after $(NMP)_{0.5}(Phen)_{0.5}(TCNQ)$ and TMTSF-TCNQ, respectively, so that comparisons of these closely related materials are easier. Even a cursory glance at Table II confirms that the predicted ρ dependence is actually observed in the CT solids. We point out, however, that rather widely different materials are being compared in Table II, and our claim is that the *predicted ρ dependence is actually obeyed more stringently than a superficial examination of Table II might suggest.* In order to arrive at this conclusion, the following very useful points are to be noted.

(i) Molecular properties, nearest-neighbor distances, and overlap patterns can be quite different in materials, and in particular, between donor and acceptor molecules. Thus the ρ dependence may be slightly blurred as we go from donor-based conductors to acceptor-based conductors. If, however, further subclassification of the materials in Table II are made—into for instance, single-chain materials based on TCNQ and its derivatives, single-chain materials based on TTF and its derivatives, two-chain ma-

terials of the TTF-TCNQ type, and so on—we see immediately how stringently the ρ dependence is obeyed within each subgroup, without even making allowances for other weaker factors.

(ii) A noticeable discrepancy is observed at $\rho=0.5$, where the behavior of $\chi_{\text{expt}}/\chi_P$ seem to be of two different types. On the one hand, in MEM(TCNQ)$_2$, DEM(TCNQ)$_2$, NMePy(TCNQ)$_2$, and its derivatives, $\chi_{\text{expt}}/\chi_P$ is $\sim$10—20, while in Qn(TCNQ)$_2$, Ad(TCNQ)$_2$, and (NMP)$_{0.5}$(Phen)$_{0.5}$(TCNQ) $\chi_{\text{expt}}/\chi_P \sim 3$. Based on our numerical calculations as well as the data for larger ρ we expect ideal chains to behave like the former group of 1:2 TCNQ salts. At present we have no theoretical explanation for this difference in behavior. However, unlike the former group of materials, the latter group exhibits a $\chi(T)$ behavior characteristic of random exchange Heisenberg chains,[47—49] and our suggestion is that the origin of the above difference lies in the weak disorder in Qn(TCNQ)$_2$, etc. This may seem contrary to what one expects from usual models of disorder, since disorder by itself causes localization and band narrowing. However, a recent investigation[61] claims that in strongly correlated bands the $2k_F$ intersite charge-density wave is enhanced by disorder. We speculate that in the magnetically disordered $\rho=0.5$ systems a weak ($\ll kT$) $2k_F$ spin-Peierls phase exists even at high temperatures, and the small magnetic gap lowers $\chi(T)$. Whether or not such a spin-Peierls phase actually exists at high temperatures will require further theoretical and experimental work, but we consider it significant that the magnitude of $\chi(T)$ at high temperatures is dependent on disorder.

(iii) In spite of the larger bandwidths in Se-based chains (and therefore a $U/t \sim 4$—5, $V_1/t \sim 2$) the ρ dependence is clear here too. This is seen most clearly from a com-

TABLE II. The peak values of the experimental magnetic susceptibilities χ_{expt} (see text), the enhancement factors $\chi_{\text{expt}}/\chi_P$ (χ_P denotes Pauli susceptibility), and the temperatures $T_{\max}$ at which the peak values are observed for representative CT solids. The abbreviations in the compound column are as follows: MEM, methylethylmorpholinium; DEM, diethylmorpholinium; NMePy, N-methylpyridine; Qn, quinolinium; Ad, acridinium; NMP, N-methylphenazine; Phen, phenazine; DCTCNQ, dichloro-TCNQ; TFTCNQ, tetrafluoro-TCNQ; TSF, tetraselenafulvalane.

Compound	ρ	χ_{expt} (emu/mole)	$\chi_{\text{expt}}/\chi_P$	$T_{\max}$ (K)
MEM(TCNQ)$_2$ [Ref. 12(a)]	0.5	2.05×10^{-3}	17.4	66
DEM(TCNQ)$_2$ [Ref. 12(b)][a]	0.5	$\sim1.1\times10^{-3}$	8.7	$\lesssim$100
NMePy(TCNQ)$_2$ [Ref. 12(c)][b]	0.5	2.75×10^{-3}	23.4	50
Qn(TCNQ)$_2$ (Refs. 47 and 48)	0.5	3.2×10^{-4}	2.75[c]	$\sim$300
Ad(TCNQ)$_2$ (Refs. 47 and 49)	0.5	3.2×10^{-4}	2.75[c]	$\sim$300
(NMP)$_{0.5}$(Phen)$_{0.5}$(TCNQ) (Ref. 49)	0.5	3.3×10^{-4}	2.75[c]	$\sim$300
NMP-TCNQ (Ref. 49)	0.67	2.2×10^{-4}	1.16	$>$300
TMTTF-bromanil [Ref. 7(c)]	0.48—0.52[d]	9.3×10^{-4}	3.9—4.1	200
TMTTF-chloranil [Ref. 7(c)]	0.54	4.66×10^{-4}	2.12	$>$300
TMTTF-TCNQ [Ref. 7(c)]	0.55	5.1×10^{-4}	2.36	$>$300
DBTTF-DCTCNQ (Ref. 60)	0.52—0.56[d]	1.2×10^{-3}	5.3—5.6	$\sim$80
TTF-TCNQ (Refs. 7, 19, and 31)	0.55—0.59[d]	6.2×10^{-4}	2.8—3.0	350
TMTSF-TCNQ (Ref. 18)	0.57	3.33×10^{-4}	1.58(2.1)[e]	$>$300
TMTSF-DMTCNQ (Ref. 31)	0.5	5.5×10^{-4}[f]	2.36(3.14)[e]	
TSF-TCNQ (Ref. 31)	0.63	3.3×10^{-4}	1.68(2.2)[e]	$>$300
HMTTF-TCNQ (Ref. 31)	0.72	2.4×10^{-4}	1.32	$>$300
HMTSF-TCNQ (Refs. 5 and 18)	0.74	1.5×10^{-4}	0.83(1.1)[e]	$>$300
TTF-Br$_{0.79}$ (Ref. 20)	0.74—0.79	0.35×10^{-4}	0.39(0.79)[e]	$>$300
Li$_x$Pt[S$_2$C$_2$(CN)$_2$]$_2$·2H$_2$O (Ref. 22)	1.18[g]	$1(0.65)\times10^{-4}$[h]	1.17(0.76)	$>$300
HMTTF-TFTCNQ (Ref. 46)	1.0	3.25×10^{-4}	2.0	$>$300

[a]Two inequivalent sheets occur in DEM(TCNQ)$_2$ [Ref. 12(b)]. We have presented only the $\chi_{\max}$ for sheet B which shows a spin-Peierls transition at 23 K. Sheet A does not undergo spin-Peierls transition down to 1.5 K. Assumption of equal bandwidths for the two sheets would indicate a more strongly enhanced χ for sheet A.

[b]Two other related materials, NMe-4MePy(TCNQ)$_2$ and NMe2,6MePy(TCNQ)$_2$ exhibit very similar $\chi(T)$ behavior [Ref. 12(c)]. (NMe4MePy is N-methyl-4-methylpyridine; NMe2,6MePy is N-methyl-2,6-dimethylpyridine.)

[c]See text for a discussion of the relatively low χ and high $T_{\max}$.

[d]The CT ρ is known to vary in these materials.

[e]The numbers in parentheses are obtained on assumption of a bandwidth of 1 eV for the donor chains. See Ref. 20 for additional discussions of the low χ in TTF-BR$_{0.79}$.

[f]This value of the susceptibility corresponds to χ(300 K) rather than $\chi_{\max}$. We have been unable to find $\chi_{\max}$ in the literature, but would expect $\chi_{\max}$ to be higher. Notice the difference between this compound and the parent compound TMTSF-TCNQ, indicating that the ρ dependence is strong even in selenium-based materials.

[g]$\chi(T)$ behavior should be similar to that of $\rho=0.82$.

[h]The larger value corresponds to the measured $\chi(T)$, while the smaller value is obtained by subtracting a Curie contribution. See Ref. 22 for details of the subtraction procedure.

parison of TMTSF-TCNQ and TMTSF-DMTCNQ in Table II. Similar difference is observed also in their x-ray scattering behavior, with $4k_F$ scattering occurring in the DMTCNQ salt, but only a $2k_F$ scattering occurring in the TCNQ salt. Comparisons of susceptibilities of TSF-TCNQ and TMTSF-TCNQ, on the one hand, and HMTSF-TCNQ, on the other hand, leads to the same conclusion. The difference between TSF-TCNQ and TMTSF-TCNQ is less striking, but this is not unexpected. In the wider band Se-based materials the transition region (between "weak" and "strong" correlation behavior) is *expected* to occur at a smaller ρ than in the S-based materials.

(iv) Our calculations are only for ρ up to 1, but due to electron-hole symmetry the behavior of $\rho > 1$ and $2-\rho$ should be the same. For $Li_x[Pt(S_2C_2(CN)_2)_2]\cdot 2H_2O$, with $\rho = 1.18$, we therefore expect small χ_{expt}/χ_ρ and large T_{max}, as indeed is the case.[22] A weakly enhanced χ and the absence of a $4k_F$ instability in this compound has been previously interpreted within the "small-U" model.[22] As we see here, an alternate explanation for these observations are possible. Further optical measurements in the low frequency (<0.5 eV) are required for choosing between the two possibilities.

(v) While most CT solids lie in the region $0.5 \leq \rho \leq 1$, a new and rather interesting series of phthalocyanine-based linear chain conductors with $\rho \sim \frac{1}{3}$ have recently been discovered. Preliminary calculations predict a strongly enhanced susceptibility for these regions. Enhancement factors of 2–3 have been reported by the investigators.[62] More recently, it has been found experimentally that ρ in these materials can be increased nearly continuously up to 1. Many of the features predicted in the present work are seen, although for a complete comparison our calculations have to be extended to $\rho < 0.5$. Experimentally, diffuse x-ray scattering data for these materials are required for further characterization.

(vi) For TTF-$Br_{0.79}$, ρ is in the regime where we expect χ_{expt}/χ_P to be relatively low. However, in this particular case $\chi_{expt} < \chi_P$. The very low (i.e., *less* than 1) enhancement factor in Table I is partly due to the fact that the true bandwidth in this material is about 1 eV (because of an eclipsed overlap of TTF molecules) rather than 0.5 eV, and partly because of the incommensurate anion potential.[20]

(vii) For several of the materials ρ is known to vary with temperature. Thus, for example, in DBTTF-DCTCNQ ρ increases from 0.52 to 0.56 from 15 to 300 K.[60] Judging from the value of χ_{max} at $T \sim 100$ K, we would predict a ρ closer to the lower value for $T \sim T_{max}$. Indeed, as we have mentioned already, such a variation in ρ adds to the steep T dependence of χ.

We have included in Table II only those materials which have been studied quite extensively and for which the degree of charge transfer is known quite precisely. In addition to these, we have examined $\chi(T)$ data for a very large number of other materials where ρ may be guessed, and these show the same trend as the materials included in Table II. These include many other 1:2 TCNQ salts, the various TTT salts, various metallomacrocyclic assemblies, and alloys of the type $(TTF)_{1-x}(TSF)_x(TCNQ)$. For the last group of materials ρ dependence of physical properties in agreement with our theoretical prediction has recently been discussed by Sakai *et al.*[63] Finally, the whole series of $(TMTSF)_2X$ and $(TMTTF)_2X$ compounds are missing in Table II; the available susceptibility data indicate that, in general, the high-temperature susceptibilities are enhanced, indicating moderate to strong Coulomb correlations for these $\rho = \frac{1}{2}$ materials. This is further indicated by the low-temperature antiferromagnetism found in some materials.[64] Mean-field theoretical results for the correlated quasi-two-dimensional spin density wave ground state may be found in the work by Yamaji.[65]

V. DISCUSSIONS AND CONCLUSIONS

Our principal purpose in the present paper was to establish that a single theoretical model, viz., the extended Hubbard model successfully explains the magnetic properties of the entire family of segregated-stack charge-transfer solids. A strong and systematic dependence of $\chi(T)$ on the charge transfer ρ is found. The entire controversy over the magnitude of the Coulomb parameters is therefore a result of not taking into account the intermolecular correlations explicitly.

In this connection several other points need be emphasized. First, explicit considerations of either the transverse transfer integral $t_\perp$ or interchain Coulomb interactions $V_\perp$ do not change our conclusions as long as $t_\perp < t$ and $V_\perp < V_\parallel$. Interchain Coulomb interactions in fact make the ρ dependence even stronger, so that the decrease of $U_{eff}(\rho)$ between $\rho = 0.5$ and 0.75 is steeper. The easiest way to see this is to again consider the limit $t = t_\perp = 0$, as in Sec. II, but now with $V_\perp > 0$, where $V_\perp$ is the nearest-neighbor interchain Coulomb interaction. Consider, for simplicity, a square lattice and the various Wigner crystal configurations that dominate the ground state in this limit. It is easily seen that for $\rho = 0.5$ a nearest-neighbor hop now has to overcome an energy barrier $V_\parallel + V_\perp$. As a result, $U_{eff}(0.5)$ *increases* with interchain Coulomb interaction. For $\rho > 0.5$, electron or hole occupancy of sites on neighboring chains cannot be perfectly off phase, and explicit considerations, as in Sec. II, show that $V_\perp$ promotes double occupancy for $\rho > 0.6$, causing a *decrease* in U_{eff}. Notice that the above statements are independent of the *sign* of $V_\perp$, and hence are true for both one-chain and two-chain systems. In general, $V_\perp$ makes the ρ dependence stronger while $t_\perp$ makes it weaker. For large enough $t_\perp$, at very low temperatures, the system can also behave quasi-two-dimensionally. The most important qualitative difference is that the SDW which decays algebraically in one dimension, can now lead to a distinct antiferromagnetic phase. From what has already been said, the tendency towards such an antiferromagnetic phase would be strongest for $\rho = 0.5$, and we believe that this is the mechanism of the SDW formation in the various $(TMTSF)_2X$ salts.[64,65]

Second, such a strong ρ dependence in $\langle n_{i\uparrow} n_{i\downarrow} \rangle / \langle n_{i\uparrow} \rangle \langle n_{i\downarrow} \rangle$ implies similar ρ dependence of long-range correlations. Thus one may expect periodicities of various charge-density waves to also reflect this behavior, as indeed is the case.[40] However, a complete theoretical in-

vestigation needs further study, since both intersite and intrasite charge-density waves can form in these systems.[42] Due to the very large Coulomb interactions in these systems, we expect not just the periodicity (i.e., $2k_F$ versus $4k_F$), but also the *nature* (i.e., intrasite versus intersite) of the dominating broken symmetries to be ρ dependent. While such a distinction may be meaningless for the highly incommensurate cases, it is important for the commensurate or nearly commensurate ρ. Thus within the extended Hubbard Hamiltonian with on-site and intersite electron-phonon interactions, one expects the *inter*site $2k_F$ charge-density wave to dominate for $\rho=1$,[66] but the *intra*site $4k_F$ CDW to be the dominating broken symmetry for $\rho=\frac{1}{2}$.[40] (Note that here we are considering only realistic relative magnitudes of U and V_1, i.e., $U>2V_1>0$. For other parameter regions, which are conceptually possible, this statement is not true.[66]) In both of these cases, we expect the charge-density waves to be accompanied by a $2k_F$ SDW.[66] Additional complications can exist, however. For example, even for the commensurate cases, the extent of coexistence of intersite and intrasite CDW can be influenced by ρ. Furthermore, the degree of coexistence is dependent also on the periodicities of the CDW's. Finally, for many real materials both periodic and random site energies are important—and at least for $\rho=1$ it has been demonstrated that there may be a broad coexistence region between intrasite and intersite CDW's in the presence of alternating site energies.[67] Presently, the possibility of simultaneous occurrence of intersite and intrasite CDW's have been investigated only for $\rho=0.5$ and 0.6,[42] while the complete ρ dependence has been investigated only for the intrasite CDW.[40] To sum up then, whether the intersite or the intrasite CDW is the dominating broken symmetry depends not only on the relative electron-phonon couplings, but also on ρ.

In this connection, an additional point needs to be made. We do not claim that the electronic Hamiltonian in Eq. (7) gives rise to the actual lattice distortions. Rather, both in the uncorrelated ($U=V_1=0$ or $U=\infty$, $V_1=0$) as well as in the correlated models, the CDW exists even when the electron-phonon coupling is zero, as may be seen from calculations of electronic susceptibilities. The CDW can then drive a periodic lattice distortion for nonzero electron-phonon coupling. Within our model the CDW is principally due to the strong nonzero nearest-neighbor interaction between electrons.[40,43]

Third, together with the $\chi(T)$ data, nuclear spin relaxation data have also been interpreted both with strong and weak correlation models.[5] In principle, these data and interpretations should be reexamined within the present context. The spin-lattice relaxation time is dependent on the wave-vector-dependent electronic susceptibility, and correlation effects on the latter have been investigated only within the random phase approximation. Recent investigations of various broken symmetries in one dimension[40,42,61,66,67] have definitely proved that such simple methods or expressions for the susceptibilities are not valid for moderate to strong Coulomb interactions. Unfortunately, however, no analytic expression for the susceptibilities exists at present. Even experimentally, the situation is not very clear as NMR relaxation studies have been performed only for a few materials. Future theoretical and experimental studies in this direction will certainly be valuable.

In conclusion, then, we have investigated the ground-state properties as well as thermodynamics of the extended Hubbard model as a function of the density ρ of electrons. A very strong ρ dependence in magnetic properties is predicted within the model. The magnetic behavior of the entire family of CT solids is shown to obey the predicted trend. The validity of the extended Hubbard model for CT solids is therefore very convincing, as none of the other electron-electron or electron-phonon coupled models predict or explain the observed trend. Experimentally, such a trend is also found in the diffuse x-ray scattering behavior.[39] Partial investigations of the latter have been performed, and more-detailed studies, as well as complete theoretical investigations of optical properties are underway.

ACKNOWLEDGMENTS

We are grateful to Dr. A. N. Bloch (Exxon Research and Engineering Company) for innumerable fruitful discussions. S.M. acknowledges valuable discussions also with Professor Z. G. Soos (Princeton University) and Dr. D. K. Campbell (Los Alamos National Laboratory). Work at Los Alamos was supported by the U. S. Department of Energy.

APPENDIX

We discuss the charge-transfer spectra of CT solids here to show how consistent values of U and V_1 are obtained even when materials with absorptions at *different* frequencies are considered. We shall first consider $\rho=1$, where an intense absorption with a band edge at ~ 5000 cm^{-1} and a peak at ~ 8000 cm^{-1} is common. This has usually been interpreted as a CT absorption within the simple Hubbard model [Eq. (2)]. Since the lowest molecular absorptions in $TCNQ^-$ and TTF^+ ions are seen at much larger frequencies, no other interpretation of the absorption at ~ 8000 cm^{-1} can be possible. This has been further confirmed by polarized reflectivity study of K-TCNQ by Yakushi *et al.*,[68] which showed that the above absorption occurs only when the polarization vector is parallel to the stacking axis of the TCNQ chain. Yakushi *et al.* have also studied the temperature dependence of the optical conductivity of this material. This latter investigation showed a narrowing of the CT absorption as well as its splitting[68] into *two* peaks at ~ 8000 cm^{-1} and $\sim 11\,000$ cm^{-1}. Furthermore, comparison of this data to that for TMB-TCNQ, in which isolated $TCNQ^-$ ion pairs are separated by TMB^+ ions, show that the peak at 11 000 cm^{-1} is absent in the latter material, and is therefore a characteristic of the infinite chain of $TCNQ^-$ ions as opposed to $TCNQ^-$ dimers.[68] The fact that the room-temperature CT absorption in $\rho=1$ materials may be a combination of two absorptions had been claimed even earlier.[69]

Clearly, in order to explain the above temperature dependence of optical conductivity, as well as the differ-

ence between $TCNQ^-$ dimers and the infinite chain, one has to go beyond the simple Hubbard model, which has only one CT absorption characteristic of both the dimer and the infinite chain. As we had discussed earlier,[6(c)] the extended Hubbard Hamiltonian very naturally explains the above observations. Intuitively, this can again be seen most easily in the $t\rightarrow 0$ limit. The ground state consists of $\cdots A^-A^-A^-A^-\cdots$, and the CT state $\cdots A^-A^-A^0A^{2-}A^-A^-\cdots$ occurs at an energy $\sim U-V_1$ relative to the ground state. For $V_1>0$, the double occupancy and the hole are bound as a CT exciton, and an additional energy V_1 is required to separate them. The two excited states are then at $\sim U-V_1$ and U, respectively, and for *finite* t transitions to even the higher-energy state are allowed, albeit with a much weaker oscillator strength.[6(c)] This was shown numerically by Bondeson and Soos.[70] Obviously, the higher-energy absorption is not expected in an isolated dimer.

Correlating the peaks in the K-TCNQ CT spectrum with $U-V_1$ and U (the band edge is expected to be at $\sim U-V_1-4t$), we then have $V_1\sim 0.4(\pm 0.1)$ eV, $U\sim 1.4(\pm 0.1)$ eV. We now discuss how the *same* values of U and V_1 are obtained even when we consider materials with $\rho<1$.

Due to the complexities of even the theoretical CT spectra within the extended Hubbard model we shall consider $\rho=0.5$ here principally. A more generalized theory for arbitrary ρ will be published separately.[43] For $\rho=0.5$, and with the approximation $U\rightarrow\infty$, the extended Hubbard Hamiltonian predicts a CT absorption with a band edge (for the rest of the discussion we shall make a distinction between the experimental band edge and the peak in absorption) at V_1-2t, provided $V_1>2t$. For *finite* U, there are two subtle differences. firstly, the critical value of V_1, at which the optical gap appears, is larger. Secondly, weaker CT absorptions are expected at a higher frequency U. Since the oscillator strengths of CT absorptions go as the reciprocal of the optical gap, we expect most of the oscillator strnegth to be in the first CT absorption. This also follows from our discussion in Sec. II. Experimentally $\rho=0.5$ materials exhibit a strong CT absorption which peaks at ~ 0.4 eV (band edge ~ 0.1—0.2 eV) and a very weak feature at ~ 1.5 eV. Correlating now the experimental band edge as $\sim V_1-2t$, the peak as $\sim V_1$, we again get a V_1 of ~ 0.4—0.5 eV. While it is tempting to explain the feature at 1.5 eV as CT absorption due to U, additional complications need to be resolved. It has, for example, been claimed that due to the interactions with the low-frequency CT absorption, the molecular absorptions in $\rho<1$ systems are red shifted to this region, and the weak feature at ~ 1.5 eV corresponds to the molecular excitation.[71(a)] Considering that the stacking axes in most TCNQ-based systems are not perpendicular to the molecular planes, this is not unreasonable. It must be pointed out, however, that the feature at ~ 1.5 eV is also present in TTF halides,[71(b)] where, (a) the stacking axis *is* perpendicular to the molecular plane, and (b) the molecular absorption occurs at a still higher frequency. Clearly, more careful polarization studies are needed to resolve the origin of the absorption at 1.5 eV. The more important point in the present context is, however, that the value of V_1 obtained from the lower-frequency absorption is *nearly identical to that* obtained from the low-temperature data for K-TCNQ crystals, even though the $\rho=0.5$ materials absorb in a very different region.

We shall only briefly mention the CT spectra for $0.5<\rho<1$. Theoretically, the oscillator strength of the absorption at $\sim V_1$ decreases, but that for a new absorption at $\sim U-2V_1$ increases with ρ (see Sec. II). Since experimentally, only one broad absorption is observed below 1 eV, and since the peak frequency is nearly the same as for $\rho=0.5$,[24(a),24(b)] we conclude that $U\sim 3V_1$ at least within the errors due to finite bandwidth effects on our analysis. Again, this fits our estimates of U and V_1.

Since the absorption at 0.4—0.5 eV (with an edge at 0.15—0.2 eV) in $\rho=0.5$ materials has also been described within electron-phonon-coupled models, we now examine the experimental situation to show that the optical gap is not induced by electron-phonon coupling. Two different kinds of electron-phonon coupling, intersite and intrasite, have been suggested as the origin of the optical gap, and both assume $V_1=0$, $U/t\rightarrow\infty$. The two models can be written as

$$H_{e\text{-ph}}^{(1)}=\sum_i [t+\alpha(u_i=u_{i+1})](c_i^\dagger c_{i+1}+c_{i+1}^\dagger c_i)\ , \tag{A1}$$

$$H_{e\text{-ph}}^{(2)}=t\sum_i (c_i^\dagger c_{i+1}+c_{i+1}^\dagger c_i)+\beta\sum_i q_i n_i\ , \tag{A2}$$

where $H_{e\text{-ph}}$ is the electronic part of the Hamiltonian, $c_i^\dagger$, c_i now refer to a *half-filled* band of spinless fermions, α and β the intersite and intrasite electron-vibration couplings, u_i the displacement of the ith molecular unit along the stacking axis, and q_i a molecular vibration [in real molecular solids, all possible molecular modes should be included in Eq. (A2)]. Both Eqs. (A1) and (A2) are expected to open an electronic gap at the Fermi surface, leading to the so-called $4k_F$ intersite $[\langle u_i\rangle=(-1)^i u_0]$ or intrasite $[\langle n_i\rangle=\rho+(-1)^i n_0]$ CDW. We shall consider these two possibilities separately.

The chief objection to the mechanism correlating optical gap to the intersite CDW is that materials with different bond-length alternation patterns absorb at nearly the same frequency. The majority of $\rho=0.5$ materials have dimerized bond alternation patterns ($4k_F$ distortion), while TEA-$(TCNQ)_2$ is tetramerized[72(a)] ($2k_F$ distortion) and $TMPD(TCNQ)_2$ has uniform nearest-neighbor TCNQ-TCNQ distances[72(b)] (TEA denotes triethylammonium; TMPD denotes tetramethylparaphenylenediamine). In spite of this, the optical gaps are nearly the same in all the above materials.[11(c),24,27,72]

The mechanism emphasizing the electron-molecular-vibration coupling has been more popular recently.[10(d),24(c)-24(d),27] We list here the reasons why this cannot be the origin of the optical gap either, although this interaction is essential for the lattice distortion. Some of the criticisms listed below apply equally to the model emphasizing the intersite CDW.

(i) A strong temperature dependence of the optical gap (both the absorption edge and the peak) is expected within the electron-phonon-coupled $U\rightarrow\infty$ models [Eqs. (A1) and (A2)], since the optical gap is directly related to the

temperature-dependent amplitude of the $4k_F$ CDW. Direct measures of the $4k_F$ intrasite CDW amplitude are the oscillator strengths of the infrared active a_g molecular modes that occur below the optical gap.[10,11,24(c),24(d),27,73] Recent measurements of the above oscillator strengths in $Qn(TCNQ)_2$ as a function of temperature[10(d)] show that the room-temperature intensities are about 25–30% of the intensities at 6 K. A concominant sharp decrease in the CT absorption frequency is expected within Eq. (A2). Experimentally, the absorption frequency is independent of temperature.[24(c)] Inclusion of a small interchain potential may be able to explain the rather slow drop in the molecular mode oscillator strengths[10(d)] [the single-chain Peierls model of Eq. (A2) predicts the gap to vanish[10(d)] at 150 K], but it still does not explain why the predicted one-to-one correspondence between the lattice distortion amplitude and the optical gap is not observed.

The above phenomenon is expected within the extended Hubbard model. Firstly, infrared active a_g modes do not prove that the optical gap is a Peierls gap ($V_1=0$), as has been claimed.[24(c)] Rather, these only prove the occurrence of a $4k_F$ CDW, which in our model is due to a strong V_1 and which can lead to lattice distortion in the presence of electron-vibration coupling. This scenario is analogous to the case of polyacetylene, where lattice distortion is present, but the optical gap can be due to the electron correlation.[66] Thus the important point in the present case is that there is now no longer a one-to-one correspondence between the a_g mode intensity and the CT absorption frequency. The lattice distortion can decrease with temperature due to a variety of reasons that decrease the effective coupling between the electrons and the lattice, but since the optical gap is due to interactions among the electrons themselves, it remains the same. To continue the analogy with polyacetylene, this is equivalent to saying that the optical gap in the latter would persist even if all bond lengths were equal. Note, however, that this decrease in lattice distortion amplitude can occur even in the presence of the CDW, as discussed in Sec. V.

(ii) An extension of the above reasoning is that in cases where the lattice distortion vanishes at a certain temperature, the optical gap should almost vanish within the electron-phonon-coupled models, but should be the same within the present model. In DBTTF-$TCNQCl_2$, $4k_F$ ordering disappears at 180 K,[60] but the optical gap is nearly the same at 100 and 300 K.[73]

(iii) Equations (A1) and (A2) both predict fractionally charged solitons or bipolarons in $\rho=0.5$ systems.[10(d),27,38] A commonly accepted signature of the such commensurability-induced defects is the so-called "midgap absorptions" that are seen in π-conjugated polymers.[2,3] In the 1:2 TCNQ salts, these defects should be generated either thermally or by adding extra electrons to the TCNQ chain [e.g., it has been claimed that the extra electrons in $(NMP)_x(Phen)_{1-x}(TCNQ)$, $0.5<x<0.57$ go to such defect levels.[38] The midgap absorptions in $(NMP)_x(Phen)_{1-x}(TCNQ)$ are expected to occur below 0.1 eV, should be observable even with the molecular modes in this region, and the overall oscillator strength of any such low-frequency mode should increase continuously with x from $x=0.5$ in $(NMP)_x(Phen)_{1-x}(TCNQ)$. However, no such midgap absorption is observed experimentally,[24(c)] even with the heavily doped system with $x\sim0.57$, in spite of the greater crystallinity of these materials compared to the π-conjugated polymers.

Within the extended Hubbard model, no new subgap transitions are expected, since all nearest-neighbor electron transfers require an energy V_1. The situation, even with $x>0.5$ in $(NMP)_x(Phen)_{1-x}(TCNQ)$, is thus analogous to polyacetylene, where the neutral soliton does not absorb at midgap.[74].

(iv) Optical gaps induced by electron-phonon coupling are expected to be much smaller in incommensurate systems than in commensurate systems, irrespective of whether $U\to0$ or $U\to\infty$. In the case of CT solids, this is not true,[24] thus again supporting the extended Hubbard model.

We believe that all of the above observations clearly indicate the shortcomings of Eqs. (A1) and (A2) as well as the necessity of including a substantial nearest-neighbor interaction in the Hamiltonian. Finally, of course, the clear and strong ρ dependence of physical properties itself is the strongest indication for a moderate V_1.

---

*Permanent address.

[1]Proceedings of the International Conference on the Physics and Chemistry of Low-Dimensional Synthetic Metals, Abano Terme, Italy [Mol. Cryst. Liq. Cryst. **119/120** (1985)].

[2]Proceedings of the International CNRS Colloquium on the Physics and Chemistry of Synthetic and Organic Metals, Les Arcs, France [J. Phys. (Paris) Colloq. **44**, C3 (1983)].

[3]Proceedings of the International Conference on Low-Dimensional Conductors [Mol. Cryst. Liq. Cryst. **77-79** (1981)].

[4]*The Physics and Chemistry of Low-Dimensional Solids,* edited by L. Alcácer (Reidel, Dordrecht, 1980).

[5]For a thorough recent review, see D. Jérome and H. J. Schulz, Adv. Phys. **31**, 299 (1982).

[6](a) Z. G. Soos, Ann. Rev. Phys. Chem. **25**, 121 (1974); (b) Z. G. Soos and D. J. Klein, in *Molecular Association,* edited by R. Foster (Academic, New York, 1974), Vol. 1, pp. 1–109; (c) S. Mazumdar and Z. G. Soos, Phys. Rev. B **23**, 2810 (1981).

[7](a) J. B. Torrance, in *Chemistry and Physics of One-Dimensional Metals,* edited by H. J. Keller (Plenum, New York, 1977), pp. 137–166. See also, J. B. Torrance, Ann. N.Y. Acad. Sci. **313**, 210 (1978); (b) J. B. Torrance, Phys. Rev. B **17**, 3099 (1980); J. B. Torrance, Y. Tomkiewicz, and B. D. Silverman, *ibid.* **15**, 4738 (1977); (c) J. B. Torrance, J. J. Mayerle, V. Y. Lee, R. Bozio, and C. Pecile, Solid State Commun. **38**, 1165 (1981). [TTF has the chemical formula $C_6H_4S_4$, with the structural formula 2,2'-bi(1,3-dithiole-2-ylidene); TCNQ has the chemical formula $C_{12}H_4N_4$, with the structural formula 2,2'-(2,5-cyclohexadiene-1,4-diylidene)bis (propanedinitide-2-ylidene).]

[8]V. J. Emery, in *Highly Conducting One-Dimensional Solids,* edited by J. T. Devreese, R. P. Evrard, and V. E. van Doren (Plenum, New York, 1979), pp. 247–303.

[9](a) A. A. Ovchinnikov, V. Ya. Krivnov, V. E. Klymenko, and

I. I. Ukrainskii, in *Organic Conductors and Semiconductors,* Vol. 65 of *Lecture Notes in Physics,* edited by L. Pál, G. Grüner, A. Jánossy, and J. Sólyom (Springer, New York, 1977), pp. 103—122; (b) J. Kondo and Y. Yamaji, J. Phys. Soc. Jpn. **43**, 424 (1977); (c) J. Hubbard, Phys. Rev. B **17**, 494 (1978).

[10](a) M. J. Rice, Phys. Rev. Lett. **37**, 36 (1976); (b) M. J. Rice, N. O. Lipari, and S. Strässler, *ibid.* **39**, 1359 (1977); (c) C. B. Duke, Ann. N. Y. Acad. Sci. **313**, 166 (1978); (d) E. M. Conwell and I. A. Howard, Phys. Rev. B **31**, 7835 (1985), and references therein. See also Synth. Met. **13**, 71 (1986).

[11](a) R. Bozio and C. Pecile, *The Physics and Chemistry of Low-Dimensional Solids,* Ref. 4, pp. 165—186; (b) R. Bozio and C. Pecile, J. Phys. C **13**, 6205 (1980); Solid State Commun. **37**, 193 (1981); (c) M. J. Rice, V. M. Yartsev, and C. S. Jacobsen, Phys. Rev. B **21**, 3437 (1980).

[12](a) S. Huizinga, J. Kommandeur, H. T. Jonkman, and C. Haas, Phys. Rev. B **25**, 1717 (1982), and references therein. See also, S. Huizinga, J. Kommandeur, G. A. Sawatzky, B. T. Thole, K. Kopinga, W. J. M. de Jonge, and J. Roos, *ibid.* **19**, 4723 (1979). (MEM^+ is N-methyl-N-ethylmorpholinium.) (b) C. F. Schwerdtfeger, S. Oostra, and G. A. Sawatzky, *ibid.* **25**, 1786 (1982), and references therein. [DEM^+ is di(N-ethyl)morpholinium.] (c) B. R. Bulka, A. Graja, and S. Flandrois, Phys. Status Solidi A **62**, K21 (1980). (NMePy is N-methylpyridine.)

[13]H. J. Schulz, Phys. Rev. B **18**, 5756 (1978).

[14]H. Gutfreund and M. Weger, Phys. Rev. B **16**, 1753 (1977); H. Gutfreund, C. Hartzstein, and M. Weger, Solid State Commun. **36**, 647 (1980), and references therein.

[15]A. N. Bloch, R. B. Weisman, and C. M. Varma, Phys. Rev. Lett. **28**, 753 (1972).

[16](a) L. I. Buravov, D. N. Fedutin, and I. F. Shchegolev, Zh. Eksp. Teor. Fiz. **59**, 1125 (1970) [Sov. Phys.—JETP **32**, 612 (1971)]; (b) A. A. Gogolin, S. P. Zolotukhin, V. I. Melnikov, E. I. Rashba, and T. F. Shchegolev, Pis'ma Zh. Eksp. Teor. Fiz. **22**, 564 (1975) [JETP Lett. **22**, 278 (1975)].

[17]S. Alexander, J. Bernasconi, W. R. Schneider, R. Biller, W. G. Clark, G. Grüner, R. Orbach, and A. Zettl, Phys. Rev. B **24**, 7474 (1981).

[18]A. N. Bloch, T. F. Carruthers, T. O. Poehler, and D. O. Cowan, in *Chemistry and Physics of One-Dimensional Metals,* edited by H. J. Keller (Plenum, New York, 1977), pp. 47—86. [TMTTF (tetramethyltetrathiafulvalene) is $(CH_3)_4C_6S_4$, or 2,2'-bi(1,3-dithiole-4,5-methyl-2-ylidene); TMTSF (tetramethyltetraselenafulvalene) is $(CH_3)_4C_6Se_4$, or 2,2'-bi(1,3-diselenole-4,5-methyl-2-ylidene.]

[19](a) E. F. Rybaczewski, A. F. Garito, A. J. Heeger, and E. Ehrenfreund, Phys. Rev. Lett. **34**, 524 (1975); (b) E. F. Rybaczewski, L. S. Smith, A. F. Garito, A. J. Heeger, and B. G. Silbernagel, Phys. Rev. B **14**, 2746 (1976); (c) E. Ehrenfreund and A. J. Heeger, *ibid.* **16**, 3830 (1977); Solid State Commun. **24**, 29 (1977); (d) J. C. Scott, A. F. Garito, and A. J. Heeger, Phys. Rev. B **10**, 3131 (1974).

[20]P. M. Chaikin, R. A. Craven, S. Etemad, S. J. La Placa, B. A. Scott, Y. Tomkiewicz, J. B. Torrance, and B. Welber, Phys. Rev. B **22**, 5599 (1980).

[21]K. Carneiro, M. Almeida, and L. Alcacer, Solid State Commun. **44**, 959 (1982).

[22]J. R. Cooper, M. Miljak, M. M. Ahmad, and A. E. Underhill, in Ref. 2, pp. 1391—1395; M. M. Ahmad, D. J. Turner, A. E. Underhill, C. S. Jacobsen, K. Mortensen, and K. Carneiro, Phys. Rev. B **29**, 4796 (1984); K. Carneiro, J. Vazquez, A. E. Underhill, and P. I. Clemensen, *ibid.* **31**, 1128 (1985).

[23]P. M. Grant, W. D. Gill, H. Morawitz, K. Bechgaard, and D. E. Sayers, Phys. Rev. B **30**, 6973 (1984).

[24](a) J. B. Torrance, B. A. Scott, and F. B. Kaufman, Solid State Commun. **17**, 1369 (1975), and references therein; (b) J. Tanaka, M. Tanaka, T. Kawai, T. Takabe, and O. Maki, Bull. Chem. Soc. Jpn. **49**, 2358 (1976); (c) K. D. Cummings, D. B. Tanner, and J. S. Miller, Phys. Rev. B **24**, 4142 (1981), and references therein; D. B. Tanner, J. S. Miller, M. J. Rice, and J. J. Ritsko, *ibid.* **21**, 5835 (1980), and references therein; R. P. McCall, D. B. Tanner, J. S. Miller, A. J. Epstein, I. A. Howard, and E. M. Conwell, in Proceedings of the International Conference on the Physics and Chemistry of Low-Dimensional Synthetic Metals, Abano Terme, Italy, Ref. 1, pp. 59—62. (d) C. S. Jacobsen, Ib Johannsen, and K. Bechgaard, Phys. Rev. Lett. **53**, 194 (1984), and references therein; C. S. Jacobsen, K. Dan. Vidensk. Selsk. Mat.-Fys. Medd., 1985.

[25](a) See, for example, Ref. 5; (b) see, for example, R. Moret and J. P. Pouget, in *Crystal Chemistry and Properties of Materials with Quasi-One-Dimensional Structures,* edited by J. Rouxel (Reidel, Dordrecht, Holland, in press), and references therein; J. P. Pouget, S. Megtert, and R. Comés, in *Recent Developments in Condensed Matter Physics,* edited by J. T. Devreese, (Plenum, New York, 1981), Vol. 1, pp. 295—309.

[26](a) E. M. Conwell, Phys. Rev. B **18**, 1818 (1978); (b) P. M. Chaikin, J. F. Kwak, and A. J. Epstein, Phys. Rev. Lett. **42**, 1178 (1979); R. C. Lacoe, G. Grüner, and P. M. Chaikin, Solid State Commun. **36**, 599 (1980); A. J. Epstein, J. S. Miller, and P. M. Chaikin, Phys. Rev. Lett. **43**, 1178 (1979).

[27]A. J. Epstein, R. W. Bigelow, J. S. Miller, R. P. McCall, and D. B. Tanner in Proceedings of the International Conference on the Physics and Chemistry of Low-Dimensional Synthetic Metals, Abano Terme, Italy, Ref. 1, pp. 43—50.

[28]T. Takahashi, D. Jérome, F. Masin, J. M. Fabre, and L. Giral, J. Phys. C **17**, 3777 (1984), and references therein.

[29]H. Gutfreund, O. Entin-Wohlman, and M. Weger, in Proceedings of the International Conference on the Physics and Chemistry of Low-Dimensional Synthetic Metals, Abano Terme, Italy, Ref. 1, pp. 457—466; M. Weger and H. Gutfreund, Comments Solid State Phys. **8**, 135 (1978), and references therein.

[30]See, for example, discussions on HMTSF-TCNQ in Ref. 5 and G. Soda, D. Jérome, M. Weger, K. Bechgaard, and E. Pedersen, Solid State Commun. **20**, 107 (1976).

[31](a) Y. Tomkiewicz, B. Welber, P. E. Seiden, and R. Schumaker, Solid State Commun. **23**, 471 (1977); (b) Y. Tomkiewicz, J. R. Andersen, and A. R. Taranko, Phys. Rev. B **17**, 1579 (1978). [TSF is $C_6H_4Se_4$, or 2,2'-bi(1,3-diselenole-2-ylidene); HMTTF ("hexamethylene"tetrathiofulvalene) is $C_{12}H_{12}S_4$, or 2,2'-bi(4,5,6-trihydro-1,3-dithiopentalene-2-ylidene); DMTCNQ is dimethyltetracyanoquinodimethane.

[32]P. Delhaes, S. Flandrois, J. Amiell, G. Keryer, E. Toreilles, J. M. Fabre, L. Giral, C. S. Jacobsen, and K. Bechgaard, Ann. N.Y. Acad. Sci. **313**, 467 (1978).

[33]J. R. Cooper, M. Weger, D. Jérome, D. Lefur, K. Bechgaard, A. N. Bloch, and D. O. Cowan, Solid State Commun. **19**, 749 (1976).

[34]P. M. Grant, W. D. Gill, H. Morawitz, K. Bechgaard, and D. E. Sayers, Phys. Rev. B **30**, 6973 (1984).

[35]T. D. Schultz and R. A. Craven, in *Highly Conducting One-Dimensional Solids,* Ref. 8, pp. 147—225.

[36]A. J. Heeger, in *Highly Conducting One-Dimensional Solids,* Ref. 8, pp. 69—145.

[37](a) R. Comès and G. Shirane, in *Highly Conducting One-*

Dimensional Solids, Ref. 8, pp. 17–67; (b) J. P. Pouget, Chemica Scr. **17**, 85 (1981); S. Kagoshima, J. P. Pouget, T. Yasunaga, and J. B. Torrance, Solid State Commun. **46**, 521 (1983); see also S. Ravy, R. Moret, J. P. Pouget, and R. Comès, Synth. Met. **13**, 63 (1986).

[38]A. J. Epstein, J. S. Miller, J. P. Pouget, and R. Comès, Phys. Rev. Lett. **47**, 741 (1981), and references therein.

[39]S. Mazumdar and A. N. Bloch, Phys. Rev. Lett. **50**, 207 (1983); A. N. Bloch and S. Mazumdar, in Proceedings of the International Conference on the Physics and Chemistry of Low-Dimensional Synthetic Metals, Abano Terme, Italy, Ref. 1, pp. 1273–1279. Very similar ideas were also put forward by S. T. Chui, Solid State Commun. **46**, 657 (1983).

[40]S. Mazumdar, S. N. Dixit, and A. N. Bloch, Phys. Rev. B **30**, 4842 (1984); Proceedings of the International CNRS Colloquium on the Physics and Chemistry of Synthetic and Organic Metals, Les Arcs, France, Ref. 2, p. 35, see also Ref. 1, **120**, 35 (1985).

[41]J. Sólyom, Adv. Phys. **28**, 201 (1979).

[42]J. E. Hirsch and D. J. Scalapino, Phys. Rev. Lett. **50**, 1168 (1983); Phys. Rev. B **27**, 7169 (1983); **29**, 5554 (1984).

[43]S. Mazumdar and S. N. Dixit (unpublished).

[44]T. Takahashi, D. Jérome, F. Masin, J. M. Fabre and L. Giral, J. Phys. C **17**, 3777 (1984); T. Takahashi, in Proceedings of the International CNRS Colloquium on the Physics and Chemistry of Synthetic and Organic Metals, Les Arcs, France, Ref. 2, p. 97; Mol. Cryst. Liq. Cryst. **120**, 97 (1985).

[45]D. J. Klein and W. A. Seitz, Phys. Rev. B **10**, 3217 (1974). See also, J. Bernasconi, M. J. Rice, W. R. Schneider, and S. Strässler, *ibid.* **12**, 1090 (1975).

[46]J. B. Torrance, J. J. Mayerle, K. Bechgaard, B. D. Silverman, and Y. Tomkiewicz, Phys. Rev. B **22**, 4960 (1980); J. B. Torrance, Y. Tomkiewicz, R. Bozio, C. Pecile, C. R. Wolfe, and K. Bechgaard, *ibid.* **26**, 2267 (1982).

[47](a) L. N. Bulaevskii, A. V. Zvarykina, Yu. S. Karimov, R. B. Lyubovskii, and I. F. Shchegolev, Zh. Eksp. Teor. Fiz. **62**, 725 (1972) [Sov. Phys.—JETP **35**, 384 (1972)]; (b) G. Theodorou and M. H. Cohen, Phys. Rev. B **19**, 1561 (1979), and references therein; (c) S. R. Bondeson and Z. G. Soos, *ibid.* **22**, 1793 (1980); (d) J. E. Hirsch and J. V. José, J. Phys. C **13**, L53 (1980). [Qn(TCNQ)$_2$ is (quinolinium)(TCNQ)$_2$; Ad(TCNQ)$_2$ is (acridinium)(TCNQ)$_2$.]

[48](a) L. C. Tippie and W. G. Clark, Phys. Rev. B **23**, 5846 (1981); (b) W. G. Clark, in *Physics in One Dimension,* Vol. 23 of *Springer Series on Solid State Sciences,* edited by J. Bernasconi and T. Schneider (Springer, Berlin, 1981).

[49]A. J. Epstein, J. W. Kaufer, H. Rommelmann, I. A. Howard, E. M. Conwell, J. S. Miller, J. P. Pouget, and R. Comés, Phys. Rev. Lett. **49**, 1037 (1982). [(NMP)$_x$(Phen)$_{1-x}$(TCNQ) is (N-methylphenazine)$_x$(phenazine)$_{1-x}$(TCNQ).]

[50]T. J. Kistenmacher, T. E. Phillips, and D. O. Cowan, Acta. Crystallogr., Sect. B **30**, 763 (1974).

[51]T. E. Phillips, T. J. Kistenmacher, A. N. Bloch, J. P. Ferraris, and D. O. Cowan, Acta Crystallogr., Sect. B **33**, 422 (1977).

[52]D. Chasseau, G. Comberton, J. Gaultier, and C. Hauw, Acta Crystallogr. Sect. B **34**, 689 (1978); T. J. Emge, D. O. Cowan, A. N. Bloch, and T. J. Kistenmacher, Mol. Cryst. Liq. Cryst. **95**, 191 (1983).

[53]D. J. Sandman, Mol. Cryst. Liq. Cryst. **50**, 235 (1979).

[54]M. Weger and H. Gutfreund, Solid State Commun. **32**, 1259 (1974).

[55]P. Bak and R. Bruinsma, Phys. Rev. Lett. **49**, 249 (1982).

[56]See, for example, U. Bernstein, P. M. Chaikin, and P. Pincus, Phys. Rev. Lett. **34**, 271 (1975).

[57]J. C. Bonner and M. E. Fisher, Phys. Rev. **135**, A640 (1964). See also Ref. 47(c) for recent references.

[58]D. K. Campbell, T. A. DeGrand, and S. Mazumdar, Phys. Rev. Lett. **52**, 1717 (1984); Proceedings of the International Conference on Semiconducting Metals ICSM 1984 [Mol. Cryst. Liq. Cryst. **118**, 41 (1985)], and unpublished.

[59]S. Kagoshima, T. Ishiguro, and H. Anzai, J. Phys. Soc. Jpn. **41**, 2061 (1976); S. K. Khanna, J. P. Pouget, R. Comès, A. F. Garito, and A. J. Heeger, Phys. Rev. B **16**, 1468 (1977).

[60]K. Mortensen, C. S. Jacobsen, A. Lindegaard-Andersen, and K. Bechgaard, in Ref. 2, pp. 1349–1352. [DBTTF ("dibutylene"tetrathiafulvalene) is $(C_4H_4)_2C_6S_4$, or 2,2′-bi(4,5,6,7-tetrahydro-1,3-dithia-2-indenylidene.]

[61]J. E. Hirsch and R. Kariotis, Phys. Rev. B **32**, 7320 (1985).

[62]For a recent review on phthalocyanine-based linear-chain conductors, see Tobin J. Marks, Science **227**, 881 (1985). See also, T. Inabe *et al.*, Synth. Met. **13**, 219 (1986).

[63]M. Sakai, S. Kagoshima, and E. M. Engler, in Proceedings of the International CNRS Colloquium on the Physics and Chemistry of Synthetic and Organic Metals, Les Arcs, France, Ref. 2, pp. 1313–1316.

[64]J. B. Torrance, H. J. Pedersen, and K. Bechgaard, Phys. Rev. Lett. **49**, 881 (1982); J. B. Torrance, in Proceedings of the International CNRS Colloquium on the Physics and Chemistry of Synthetic and Organic Metals, Les Arcs, France, Ref. 2, pp. 799–804.

[65]K. Yamaji, J. Phys. Soc. Jpn. **54**, 1034 (1985). See also, Synth. Met. **13**, 29 (1986).

[66]S. N. Dixit and S. Mazumdar, Phys. Rev. B **29**, 1824 (1984); S. Mazumdar and D. K. Campbell, Phys. Rev. Lett. **55**, 2067 (1985).

[67]S. Mazumdar and S. N. Dixit, Phys. Rev. B **29**, 2317 (1984).

[68]K. Yakushi, T. Kusaka, and H. Kuroda, Chem. Phys. Lett. **68**, 139 (1979).

[69]D. B. Tanner, C. S. Jacobsen, A. A. Bright, and A. J. Heeger, Phys. Rev. B **16**, 3283 (1976); W. A. Bryden *et al.* (unpublished).

[70]S. R. Bondeson and Z. G. Soos, Chem. Phys. **44**, 403 (1979). See also, S. K. Lyo, Phys. Rev. B **18**, 1854 (1978).

[71](a) K. Yakushi, M. Iguchi, G. Katagiri, T. Kusaka, T. Ohta, and H. Kuroda, Bull. Chem. Soc. Jpn. **54**, 348 (1981); A. Graja and R. Swietlik, J. Phys. (Paris) **46**, 1417 (1985). (b) J. B. Torrance, B. A. Scott, B. Welber, F. B. Kaufman, and P. E. Seiden, Phys. Rev. B **19**, 730 (1979).

[72](a) A. Filhol and M. Thomas, Acta Crystallogr., Sect. B **40**, 44 (1984); J. P. Farges, J. Phys. (Paris) **46**, 465 (1985), and references therein; (b) R. Somoano, V. Hadek, S. P. S. Yen, and A. Rembaum, J. Chem. Phys. **62**, 1061 (1975).

[73]C. S. Jacobsen and K. Bechgaard, in Proceedings of the International Conference on the Physics and Chemistry of Low-Dimensional Synthetic Metals, Abano Terme, Italy, Ref. 1, **120**, 71 (1985).

[74]Z. G. Soos and L. R. Ducasse, J. Chem. Phys. **78**, 4092 (1983); B. R. Weinberger, C. B. Roxlo, S. Etemad, G. L. Baker, and J. Orenstein, Phys. Rev. Lett. **53**, 86 (1984).